Università degli Studi di Cagliari

DOTTORATO DI RICERCA

Ingegneria Industriale

Ciclo XXIX

TITOLO TESI

ELECTROLYSIS OF WATER CONTAINING MICROALGAE FOR REMOVAL OF HARMFUL SPECIES AND PRE-TREATMENT OF MICROBIAL FUEL CELL FEED

Settore scientifico disciplinari di afferenza

ING-IND/25 IMPIANTI CHIMICI

Presentata da:	Sara Monasterio Martinez
Coordinatore Dottorato	Francesco Aymerich
Tutor	Michele Mascia

Esame finale anno accademico 2015 – 2016
Tesi discussa nella sessione d'esame marzo – aprile 2017

Acknowledgements

I would like to express my special appreciation and thanks to my supervisor, Prof. Michele Mascia, for the possibility of undertaking this PhD, and for the support and advice he gave me during these three years of research at the Department of Mechanical, Chemical Engineering and Materials (DIMCM), University of Cagliari, Italy.

I would like to thank Prof. Annalisa Vacca and Prof. Simonetta Palmas for their assistance and guidance throughout my research years.

I would also like to thank my English co-supervisor, Dr. Mirella di Lorenzo, for her help during my stay at the University of Bath, United Kingdom.

Thanks to Pablo for his affection, for the hand that he extended me in difficult times and for the things he shared with me inside and outside the University.

Finally, special thanks to my family for the unconditional support they provided me during my academic training and therefore, for achieving this goal.

Contents

Abstract

In the present project, an experimental work is presented about the electrolysis of water containing harmful microalgae and pre-treatment of microbial fuel cell feed. The work has been carried out at the laboratory of Electrochemical Engineering under the supervision of Prof. Michele Mascia of the Department of Mechanical, Chemical Engineering and Materials, University of Cagliari, and under the supervision of Dr. Mirella Di Lorenzo at the laboratories of the Bioprocessing Research Unit of the Department of Chemical Engineering, University of Bath.

Uncontrolled algal growth in water systems causes a number of serious issues that range from unpleasant odors and tastes to eutrophication. *Microcystis aeruginosa*, a blue-green alga, and *Chlorella vulgaris*, a green one, were adopted as the model microalgae. A fixed bed electrochemical reactor in flow was tested, which was equipped with three-dimensional electrodes constituted by stacks of grids electrically connected in-series, with the electric field parallel to the fluid flow. Nb grids coated with conductive diamond and titanium grids coated with Ir/Ru mixed oxides were used as anode packing, while titanium grids coated with platinum as cathode one.

The reactor was characterised for mass transfer, by the limiting current densities techniques, and flow behavior, by pulse-response curves with an inert tracer. Electrolysis experiments were carried out in continuous and in batch recirculated mode with flow rates corresponding to *Re* from 10 to 80, Cl^- concentrations up to 600 mg dm^{-3}, and current densities ranging from 10 to 60 A m^{-2}. The absorbance of chlorophyll-*a* pigment and the concentration of products and by-products of electrolysis were measured.

A simple plug flow mathematical model at steady state was implemented, combining the pseudo-first order kinetics, describing chemical and electrochemical reactions, with the axial dispersion, which accounts for the

non-ideal flow behavior of the system. The model allowed obtaining the concentration profiles of chloride and chloride oxidation by-products, which were compared with experimental data, with good agreement in a wide range of flow rates. The model was also successfully used to simulate the performance of the reactor in the single-stack configuration used for the experiments and in multi-stack configurations.

In this present study, first laboratory-scale preliminary results for a cost-effective and green solution to the treatment of algae contaminated water systems are also given since current methodologies to treat algae are costly and require harsh chemicals.

In particular, an integrated closed-loop system that combines the electrolysis unit with a stack of miniature single chambered air-cathode microbial fuel cells (MFCs) for the treatment of algae contaminated wastewater and energy generation is reported. The effect that MFC design and number of MFC units in the stack have on performance was investigated. Guidelines on the system optimisation are therefore also provided.

This work is believed to be a first step towards an effective removal of microalgae that is not only self-sustainable but can also generate extra useful energy.

Chapter 1

Overview of the Thesis

1.1. Motivations

Microalgae are unicellular species, which can exist either as a single cell or as colonies. Algae are usually found in tropical and semi-tropical areas, especially, in freshwater and marine systems. As a result of the release of waste from domestic, agricultural and industrial activities in water systems, they can grow excessively under high nutrients contents in surface waters. The high concentrations of nitrogen and phosphorous may give the ideal medium for the massive growth of algae, which causes explosive proliferations of plants and algae that are commonly known as eutrophication.

The presence of algae in water can negatively influence on drinking water quality and on conventional water treatment processes. In fact, some species can release toxins in water as cyanotoxins. This kind of toxins are usually liberated by the cyanobacteria specie and may constitute a serious risk for health and environment. Moreover, if contained in high concentrations, these substances can be toxic and dangerous to humans, but also under the lethal dose, cyanotoxins in drinking water are implicated as one of the key risk factors for the high occurrence of primary liver cancer. Furthermore, the water contaminated with toxic cyanobacteria also might cause the death of domestic and wild animals. These toxins are commonly released into water following the cyanobacterial cell lysis, which often happens during their passage through a conventional water treatment plant.

Thus, the removal of algae from wastewater has then gained importance in recent years. However, due to their small size and low specific gravity, it is difficult to remove algae effectively with conventional processes of water treatment, such as sedimentation or filtration. Therefore, the interest on electrochemical oxidation procedures has increased for the treatment of wastewater because it is relatively economical, has higher treatment efficiency, and does not require storage of chemicals. Additionally, the construction of the reactors and managements are simples, which makes it suitable for automation.

On this basis, an alternative to traditional disinfection processes may be the water disinfection by direct electrolysis, which combines the

electrochemical process of disinfectant production with the treatment process in a single unit. In this process, algae may behave as colloidal particles and can be separated from water solution by the applied electric field. The removal efficiency of the process can be related to the synergistic effect of electrogenerated oxidants, applied electric field on the cell membrane and pH gradients in the reactor. Moreover, when the electrolyte contains Cl^- ions, different disinfecting agents (depending on the anode material employed) can be formed during electrolysis of water, such as reactive oxygen species and chlorinated compounds that can successfully inactivate the bacteria.

The effectiveness of the disinfection process, regarding the high bactericidal effect, is based mostly on the anode material, hydrodynamics, electric potential and reactor configuration. These parameters should also be carefully established so as to avoid the formation of undesired by-products, such as chlorates and/or other chloride oxidation products.

As the cell configuration is concerned, in addition to the working conditions, three dimensional electrodes have gained great attraction for electrochemical treatment of waters since high specific areas, high mass transfer rate and low reaction volumes are desired. So far, no papers focused on the investigation of three-dimensional electrodes for the disinfection of water employing a low chloride amount are found. Therefore, the configuration proposed in this project is constituted by a flow through tubular reactor with three-dimensional electrodes, in which both anode and cathode packings are arranged in 6 discs in-series.

Nb grids coated with conductive diamond (BDD) and expanded meshes of commercial Ir/Ru mixed oxides (dimensionally stable anodes, DSA) constituted the anode packing. In this case, a surface effect may also be considered, depending on the anode material, which in turn determines the nature of the surface oxidants: at BDD the formation of oxygenate radicals, transient of water oxidation to oxygen, occurs, while the formation of superior oxides is the main mechanism at DSA.

The reactor was tested in continuous and in batch recirculated electrolysis of water containing *Microcystis aeruginosa* and *Chlorella vulgaris*

microalgae with Cl^- ions concentrations up to 600 mg dm^{-3}. The hydrodynamics of the reactor was characterised by pulse-response tests with inert tracer and the mass transfer characterisation study with the standard redox ferricyanide/ferrocyanide couple.

The effects of applied current density, flow rate and inlet chlorides concentration on the removal of the two microalgae above mentioned, by means of the chloride-oxidation products concentration inside the reactor and in the outlet stream, were investigated.

Steady state data was quantitatively interpreted by a mathematical model by combining the main kinetic equations with an axial-dispersed plug flow model, which accounts for the non-ideal flow conditions. The model allowed obtaining the concentration profiles of chloride and chloride oxidation by-products, which were compared with experimental data in a wide range of flow rates. The model was also successfully employed to simulate the behavior of the reactor in the single-stack configuration used for the experiments and in multi-stack configurations.

On the other hand, the main drawback of the electrolysis is, however, directly related to its energy requirements, which would add to the great amount of energy that water treatments require. Nevertheless, the direct electrolysis of microalgae leads to the release of intracellular matter, such as lipids, which could be exploited as fuel in microbial fuel cells (MFCs) to produce useful electricity.

MFCs have attracted a lot of attention in the past decade as innovative renewable and carbon-neutral bio-electrochemical devices, capable of generating energy from waste water effluents through the action of electroactive microorganisms while treating waters.

On theses basis, and with the aim to transform the way we perceive wastewater by converting it from an energy issue to an energy source, the two processes were linked up. Specifically, a closed-loop system was tested in which the electrolysis reactor was coupled to a cascade of 3 to 5 single chambered air-cathode MFCs hydraulically arranged in-series. The MFCs

in the stack were electrically independent from each other to monitor individually their performance.

This integrated approach for the wastewater treatment is not only chemical-free but it also intends to be energy-neutral. As such, the approach: is sustainable and environmentally friendly; does not require further treatments associated to the use of chemicals; and does not require extra energy.

1.2. Summary

This Thesis is structured in two main chapters, each one subdivided in 3 sections in order to allow the reader to better follow the development of the research project. The subdivided sections are organised as follows: introduction, materials and methods, and results and discussion. Conclusions are reported in a separate chapter.

Supporting materials, such as supplemental text, tables, and figures, can be found in the Appendix.

A summary of this Thesis is shown in the following list, where a brief description of each chapter and section is given.

Chapter 2. Electrolysis of water containing *Microcystis aeruginosa* and *Chlorella vulgaris* in a fixed bed reactor with 3D electrodes

2.1. Introduction I

The objectives of the work and an adequate background, providing a detailed literature, about an electrochemical treatment as a pre-oxidative step in a process to inactivate *Microcystis aeruginosa* and *Chlorella vulgaris* algae at relative high concentrations, in order to simulate the conditions occurring in aquatic systems and harmful for bloom formation, are given.

2.2. Materials and methods I

The procedures to obtain the experimental data used to study the electrochemical removal of *Microcystis aeruginosa* and *Chlorella vulgaris* algae are explained as well as all devices used. The techniques used to characterise the electrochemical reactor are also described.

2.3. Results and discussion I

The effect of the electrolyte's residence time inside the electrochemical reactor, the current density, the inlet chloride ions concentration and the anode material employed on the electrolysis process is a key factor in controlling algal biomass in aqueous media. Therefore, experimental results obtained for the electrochemical removal of *Microcystis aeruginosa* and *Chlorella vulgaris* algae at the relevant operative conditions are reported and are also discussed clearly and concisely.

Chapter 3. An integrated electrolysis-microbial fuel cell closed-loop system for *C. vulgaris* algae removal in water

3.1. Introduction II

The objectives of the work and an adequate background, giving some detailed citations, about providing a cost-effective and green solution to the treatment of *Chlorella vulgaris* algae contaminated water systems by the integration of the electrolysis reactor with a stack of miniature microbial fuel cells for the treatment of algae contaminated water and energy generation is introduced.

3.2. Materials and methods II

The procedures to obtain the experimental data used to investigate the removal of *Chlorella vulgaris* in the integrated process studied, which combines the electrolysis unit with a stack of miniature single-chambered air-cathode microbial fuel cells, are explained as well as all devices used.

3.3. Results and discussion II

This section discusses clearly and concisely the preliminary experimental results for the first integrated system that combines the electrolysis reactor with a stack of miniature microbial fuel cells for the treatment of *Chlorella vulgaris* algae contaminated water and energy generation. The effect that microbial fuel cell design and number of microbial fuel cell units in the stack have on performance is also reported.

Chapter 4. Conclusions

Main conclusions of the electrochemical removal of *Microcystis aeruginosa* and *Chlorella vulgaris* algae from water in a packed bed reactor constituted by three-dimensional electrodes and of the integration of the plug flow electrochemical reactor with a stack of miniature air-cathode microbial fuel cells for the *Chlorella vulgaris* algae treatment in water and energy generation are reported.

Appendix. This chapter is focused on providing further information about the electrochemical techniques used to investigate the mass transfer characterisation and the model equations employed in the electrochemical process for algae inactivation.

1.3. Publications in Journal and Conference Papers

Some of the work present in this Thesis has been published in international journal papers, national and international congresses.

International Journal Papers:

M. Mascia, S. Monasterio, A. Vacca, S. Palmas, *Electrochemical treatment of water containing Microcystis aeruginosa in a fixed bed reactor with three-dimensional conductive diamond anodes*, J. Hazard. Mater. 319 (2015) 111-120. doi:10.1016/j.jhazmat.2016.03.004.

S. Monasterio, F. Dessì, M. Mascia, A. Vacca, S. Palmas, *Electrochemical removal of Microcystis aeruginosa in a fixed bed reactor*, Chem, Eng. Trans. 41 (2014) 163–168. doi:10.3303/CET1441028.

Not yet published International Journal Papers:

S. Monasterio, M. Mascia, M. Di Lorenzo, *Electrochemical removal of Chlorella vulgaris with an integrated electrolysis-microbial fuel cell closed-loop system* [Submitted to "Separation and Purification Technology"].

National and International Congresses and Conferences:

S. Monasterio, M. Mascia, A. Vacca, S. Palmas, *Engineering of electrochemical processes for water treatment in a fixed bed reactr with conductive diamond anodes*, Convegno Gricu 2016, Anacapri (Italy), September 2016.

S. Monasterio, M. Mascia, M. Di Lorenzo, A. Vacca, S. Palmas, *A cascade of miniature microbial fuel cells coupled with an electrochemical reactor for energy harvesting*, European Fuel Cell Technology and Applications, Naples (Italy), December 2015.

S. Monasterio, A. Vacca, S. Palmas, M. Mascia, *Kinetics of electrochemical removal of Microcystis aeruginosa from natural waters with DSA and BDD anodes*, ECCE10, Nice (France), September 2015.

S. Monasterio, F. Dessì, M. Mascia, A. Vacca, S. Palmas, *Electrochemical removal of Microcystis aeruginosa in a fixed bed reactor*, 10th European Symposium on Electrochemical Engineering, Chia, Sardinia (Italy), October 2014.

S. Monasterio, F. Dessì, M. Mascia, A. Vacca, S. Palmas, Electrochemical treatment for the removal o*f Chlorella vulgaris and Microcystis aeruginosa by using a fixed bed cell*, 65th Annual Meeting of the International Society of Electrochemistry, Lausanne (Switzerland), September 2014.

S. Monasterio, F. Dessì, M. Mascia, A. Vacca, S. Palmas, *Electrochemical removal of microalgae from water in a fixed bed reactor with three dimensional electrodes*, XXXV RGERSEQ-1st E3, Burgos (Spain), July 2014.

In addition to the work presented in this Thesis the author has also participated, during the course of the study, in other research projects:

International Congresses and Conferences:

P. Ampudia, S. Palmas, A. Vacca, M. Mascia, L. Mais, S. Monasterio, S. Rizzardini, E. Musu, *Systematic investigation on the effect of the synthesis conditions on the performance of nanotubular structured electrodes,* SiO_2 Advanced dielectrics and related devices, X International Symposium, Cagliari (Italy), June 2014.

Chapter 2

Electrolysis of water containing *Microcystis aeruginosa* and *Chlorella vulgaris* algae in a fixed bed reactor with 3D electrodes

2.1. Introduction I

2.1. Introduction I

Algae in water are of great concern because they can adversely affect drinking water quality and water treatment processes [1,2]. The release of waste from domestic, agricultural and industrial activities in water systems can lead to extremely high concentrations of nutrients and cause explosive proliferations of plants and algae up to eutrophication. The uncontrolled growth of algae (blooms) affects the taste and odour of drinking water and can lead to the generation of toxins that critically compromise its safety.

Cyanobacteria, usually known as blue-green algae, are commonly located across all latitudes in freshwater and in marine water. These kind of species can produce and release toxins in water which, in the presence of blooms, may reach prejudicial concentrations for health and environment [3–5].

A well-known bloom-forming cyanobacterium is *Microcystis aeruginosa* (*M. aeruginosa*), which is a blue-green photoautotrophic gram-negative microalga with a spherical shape 3.0–7.0 µm in diameter and with a specific gravity of 1200 kg m^{-3}. *M. aeruginosa* is considered the most common toxic cyanobacteria in eutrophic freshwater, which can lead to the release of heptapeptides and neurotoxins in water systems in the form of microcystins (MCs) and cyanopeptolins due to its uncontrolled growth [6–8].

Green algae *Chlorella vulgaris* (*C. vulgaris*) was also adopted as an algal model since it represents one of the 8 species of *Chlorella*. *C. vulgaris* has been found in surface waters worldwide as lakes, reservoirs, shores of ponds and slow-moving rivers [9], and it is considered a genus of single-cell green algae with a spherical shape (2.0–10.0 µm in diameter) [10].

Many studies have been devoted to the possibility of controlling the extensive growth of algae in reservoirs and lakes by the addition of plant hormones, lime, alum, copper sulfate or potassium permanganate [2,11,12].

The presence of microalgae in conventional water treatment processes may cause different issues, such as the clogging of intake screens and filters, the disruption of floc settling, the fouling of weirs and the appearance of algal mats [13]. Therefore, different processes have been suggested to prevent the eutrophication, such as sand filtration and coagulation [13–16]. As

alternative techniques, electrocoagulation-electroflotation combined treatment was proposed; better results were obtained using aluminium electrodes rather than iron electrodes [17,18]. The main disadvantage of electrocoagulation is the need to regularly replace the sacrificial anode in order to avoid the increase of electrical consumption and the decrease of process efficiency [19]. Direct electrolysis (DE), as a pre-oxidative step towards algae inactivation, was investigated for disinfection, with efficiencies dependent on the microorganisms considered. The effectiveness of the process has been directly correlated to oxidants electrogenerated, extreme pH conditions and electric field [20–23].

To the best of our knowledge, not many studies exist on the use of electrolysis for the *in situ* generation of oxidants with the aim of controlling algal concentration in aqueous media. Xu et al. [24] and Liang et al. [25] have studied the inhibition of *M. aeruginosa* growth by electrolysis using Ti/RuO_2 anodes. In a previous work carried out in our laboratory, the inactivation of *Chlorella vulgaris* has been investigated with conductive diamond anodes in a filter-press reactor [26].

In this work, the results of an experimental investigation are presented in which DE at Nb grids coated with conductive diamond (BDD) and titanium grids coated with Ir/Ru mixed oxides (DSA), used as anodic material, are adopted to study the treatment of water containing *M. aeruginosa* and *C. vulgaris*.

As it is widely discussed in the literature, during the electrolysis of water with conductive diamond and Ir/Ru mixed oxides electrodes, several electrochemical and chemical reactions occur. In this case, a surface effect may also be considered depending on the anode material employed. This surface effect determines the nature of the surface oxidants: the very high overpotential for the oxygen evolution at BDD anodes favours the oxidation of chlorides to active chlorine with respect to the generation of oxygen radicals [27], while the formation of superior oxides is the main mechanism at DSA.

During electrolysis of water with BDD anodes different oxidants at the electrode surface can be formed. Depending on their reactivity, these

oxidants may be effective in a thin reaction film adjacent to the electrode surface (pseudo-surface oxidants) or in the bulk. Different works have been devoted to the description of these reactions at BDD anodes and the main are summarised in *Table 1*.

Table 1. *Main reactions occurring during electrolysis of water with BDD anodes.*

r1	$H_2O \rightarrow OH^- + H^+ + e^-$	r 13	$HClO + 2OH^\bullet \rightarrow HClO_2 + H_2O$
r2	$OH^- \rightarrow OH^\bullet + e^-$	r 14	$HClO_2 + 2OH^\bullet \rightarrow HClO_3 + H_2O$
r 3	$OH^\bullet \rightarrow O^\bullet + H^+ + e^-$	r 15	$HClO_3 + 2OH^\bullet \rightarrow HClO_4 + H_2O$
r 4	$H_2O_2 \rightarrow O_2 + 2H^+ + 2e^-$	r 16	$ClO^- + OH^\bullet \rightarrow ClO_2^- + H^+ + e^-$
r 5	$2O^\bullet \rightarrow O_2$	r 17	$ClO_2^- + OH^\bullet \rightarrow ClO_3^- + H^+ + e^-$
r 6	$2OH^\bullet \rightarrow H_2O_2$	r 18	$ClO_3^- + OH^\bullet \rightarrow ClO_4^- + H^+ + e^-$
r 7	$O_2 + O^\bullet \rightarrow O_3$	r 19	$2ClO_2 + H_2O \rightarrow ClO_2^- + ClO_3^- + 2H^+$
r 8	$2SO_4^{2-} + 2OH^\bullet \rightarrow S_2O_8^{2-} + 2OH^-$	r 20	$3ClO^- \rightarrow ClO_3^- + 2Cl^-$
r 9	$2Cl^- \rightarrow Cl_2 + 2e^-$	r21	$H_2O + e^- \rightarrow 0.5H_2 + OH^-$
r 10	$Cl_2 + H_2O \leftrightarrow HClO + Cl^- + H^+$	r22	$ClO^- + 2e^- \rightarrow Cl^- + OH^-$
r 11	$HClO \leftrightarrow ClO^- + H^+$	r23	$2H_2O + ClO_2 + 5e^- \rightarrow Cl^- + 4OH^-$
r 12	$3OH^\bullet + HClO \rightarrow ClO_2 + 2H_2O$		

Electrochemical oxidation of water at BDD produces hydroxyl radicals and other highly reactive radicals (r1–r3), which can be effective only in a thin layer adjacent to the anode surface: the reactions involving these species are then pseudo-surface reactions [28–30]. The pseudo-surface oxidants may react with water or transients of water oxidation, to give oxygen (r4, r5) or bulk oxidants, such as hydrogen peroxide or ozone (r6, r7) [31]. In the presence of sulfates, the mechanism of the formation of persulfate is well known (r8) [32–34]; only HSO_4^- and undissociated H_2SO_4 react with $^\bullet OH$ radicals to form sulphate radicals. At neutral pH, the main form of

sulphate is SO_4^{2-}, being the concentration of undissociated H_2SO_4 negligible. Consequently, the production of SO_4^{2-} and $S_2O_8^{2-}$ is not significant in this study.

When the electrolyte contains chlorides, the oxidation to active chlorine species, such as dissolved chlorine, hypochlorous acid, hypochlorite ions and chlorine dioxide may occur (r9–r12). These species are also bulk oxidants, but they can react with bulk and surface oxygen species (r13–r19) to give undesired by-products; these by-products may be chlorite, chlorate and perchlorate, depending on the inlet concentration of Cl^- ions and on the operative conditions: deactivation of active chlorine has been also observed (r19–r20) [35–39].

During electrolysis of water with DSA electrodes, however, two main reactions occur at the anode surface: adsorbed and dissolved chlorine are generated from the oxidation of chloride ions (r9), while oxygen evolves from water discharge:

$$2H_2O \rightarrow O_2 + 4H^+ + 4e^- \quad (1)$$

The dissolved chlorine, formed by the electrochemical reaction (r9), may in turn react with water to give hypochlorous acid (r10) and hypochlorite ions (r11). The distribution of the three forms of active chlorine depends on the conditions, at the neutral or weakly alkaline pH of the water processed in the electrolyses, the reaction of disproportionation is shifted towards HClO.

Under particular operative conditions, in weakly alkaline media chlorates can be formed following the well-known electrochemical Foerster reaction:

$$2HClO + ClO^- \rightarrow ClO_3^- + 2Cl^- + 2H^+ \quad (2)$$

The formation of chlorate may be also electrochemically generated at RuO_2/TiO_2 anodes from the hypochlorite oxidation (equation (3)) and by direct electrochemical oxidation of chloride without a dissolved hypochlorite as intermediate and the conversion of hypochlorite (equation (4)) [40].

$$6HClO + 3H_2O \rightarrow 2ClO_3^- + 4Cl^- + 12H^+ + 3/2O_2 + 6e^- \quad (3)$$

$$Cl^- + 3H_2O \rightarrow 2ClO_3^- + 6H^+ + 6e^- \quad (4)$$

At the cathode the main reactions are the hydrogen evolution (r21) and the reduction of active chlorine to chloride ions (r22): the electrochemical reaction of the active chlorine reduction is fast, so that the kinetic of active chlorine reduction may be assumed controlled by the mass transfer towards the cathode surface [39].

In previous studies carried out under conditions similar to the ones here adopted, active chlorine species were found to be the main components of the mixture [26,39,41,42].

As the reactor configuration is concerned, 3D electrodes were proposed to obtain high space-time yield in processing dilute solutions, where high specific area and high mass transfer rate are requested [43]. The fixed bed electrochemical cell here adopted was tested for the treatment of low conductive waters, showing high suitability for primary and secondary disinfection [44].

The present study investigated the electrochemical treatment as a pre-oxidative step in a process to inactivate *M. aeruginosa* and *C. vulgaris* at relative high concentrations (in the order of 10^6 cells dm^{-3}), in order to simulate the conditions occurring in aquatic systems and harmful for bloom formation [45]. The operating conditions for the treatment of water with low content of algae were determined and the relative experiments were performed in a fixed bed electrochemical reactor equipped with three-dimensional anodes. Runs were carried out either in a single pass configuration, in continuous mode, or in a recirculated system with reservoir, in batch recirculated mode when BDD anodes were tested, while in continuous mode for DSA anodes.

Data from continuous experiments were modelled through a simple dispersed plug flow model, combined with the kinetic equations of the different reactions occurring in the system.

2.2. Materials and methods I

2.2. Materials and methods I

2.2.1. Algae culture

M. aeruginosa and *C. vulgaris* microalgae were acquired from SAG (Georg-August Göttingen University, Germany). BG 11 medium was employed for the microalgae cultivation, with the following composition (all values in mg dm^{-3}): $NaNO_3$ 1500; $K_2HPO_4 \cdot 3H_2O$ 40; $MgSO_4 \cdot 7H_2O$ 75; $CaCl_2 \cdot 2H_2O$ 36; citric acid 6; ferric ammonium citrate 6; EDTA (disodium-salt) 1; Na_2CO_3 20; and 1 cm^3 dm^{-3} of a solution containing (g m^{-3}): H_3BO_3 61; $MnCl_2 \cdot 4H_2O$ 197; $ZnSO_4 \cdot 7H_2O$ 287; $CuSO_4 \cdot 5H_2O$ 2.5; $(NH_4)_6Mo_7O_{24} \cdot 4H_2O$ 12.5. Both microalgae were cultivated under fluorescent light at room temperature (25 ± 1°C) in glass flasks containing each one a litter of BG 11 medium and adjusted to pH 7.0 by the addition of HCl (0.1 M). An example of a typical curve of the algal growth is reported in *Figure 27A* (see Appendix (I)). The conductivity of the solution was about 4 ± 2 mS cm^{-1}. Experiments were performed when algae were in the *log-growth* phase, which corresponded to a concentration of algae of 10 × 10^9 cells dm^{-3}.

2.2.2. Electrochemical cell

DE experiments were performed with the fixed bed electrochemical reactor previously developed [44]. The cell was made of Plexiglas with a cylindrical shape constituted of a single compartment with an inner diameter (d) of 5 cm and a height of 15 cm (*Figure 1A*). The cell was equipped with 3D electrodes consisted either of six discs in-series of niobium grids coated with conductive diamond (BDD) or titanium grids coated with Ir/Ru mixed oxides (DSA) in the case of the anode packing, while six discs in-series of titanium grids coated with platinum for the cathode one. Details of a typical grid are shown in *Figure 1B*. The solid surface (A) of both electrodes was 100 cm^2. The anode packing was placed 6.5 cm far from the inlet section, and the inter-electrode gap was approximately 0.5 cm wide. The resulting reactor was filled with glass spheres (d_p = 0.2 cm) leading to a bed void fraction (ε) of 0.36, and a liquid volume (V_R) of 100 cm^3. Sampling ports were located at the bottom, the inter-electrode gap and the top of the reactor.

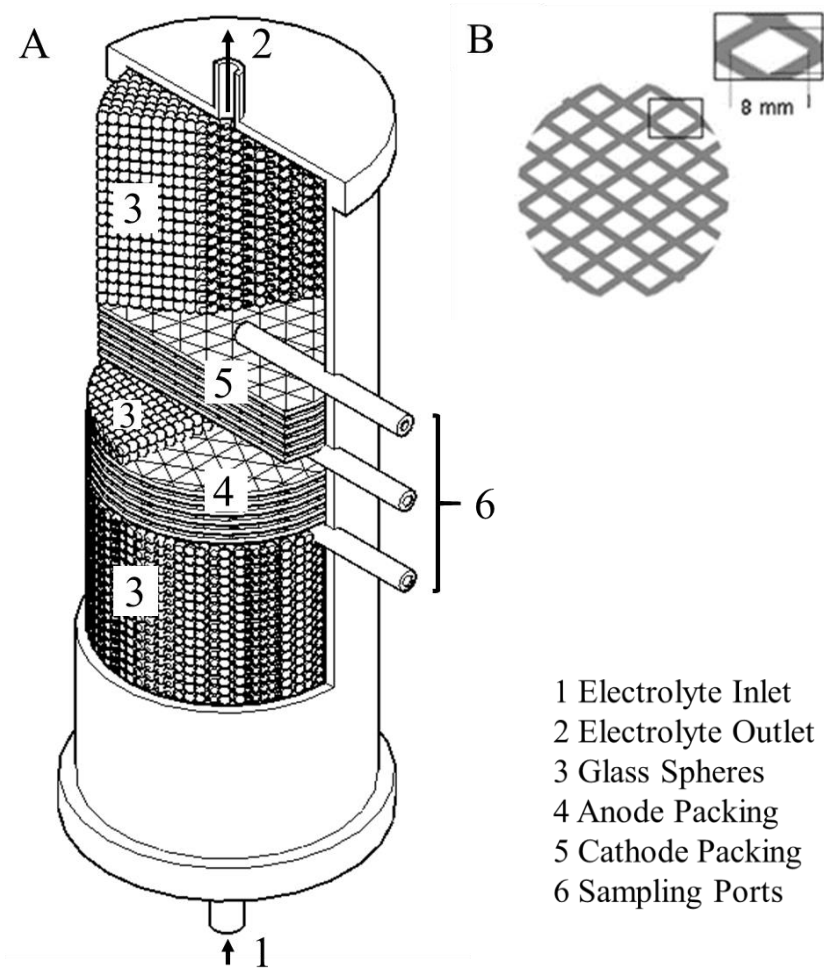

Figure 1. *Experimental apparatus for the direct electrolysis. (A): axonometric sketch of the electrolysis reactor, showing the stacks of grids that constitute the anode and cathode packing, the inert filling (glass spheres) and the inlet and outlet. (B): details of a grid.*

2.2.3. Electrolysis experiments

The cell was used both in batch recirculated mode and in continuous mode. In the batch recirculated electrolyses (*Figure 2A*), the cell was inserted in a hydraulic circuit and the electrolyte was pumped by a peristaltic pump (ISM-010) from the reservoir to the cell and back with recirculating flow rates ranging between 25 and 200 cm^3 min^{-1}, which corresponded to Reynolds (*Re*) values 10 and 80, respectively: the volume of the system (*V*) was 300 cm^3. In the continuous experiments (*Figure 2B*), the electrolyte was pumped by the peristaltic pump and flowed throughout the cell in a single pass mode, with hydraulic residence time ($\tau = V_R/Q$) variable from 15 (*Re* = 160) to 240 s (*Re* = 10). *Re* values were calculated employing the reactor inner diameter, *d*, as characteristic length.

A current supply was connected to the electrodes, with the electric field parallel to the fluid flow, and batch recirculated and continuous electrolyses of the BG 11 media in the presence or absence of microalgae were operated under fixed current density (*i*) values ranging from 10 to 60 A m^{-2} by means of a galvanostat (AMEL-2049). The resulting cell voltage was between 7 and 20 V. Depending on the runs, sodium chloride was added to the solution up to a final concentration, in the inlet stream of the reactor, of 600 mg dm^{-3}.

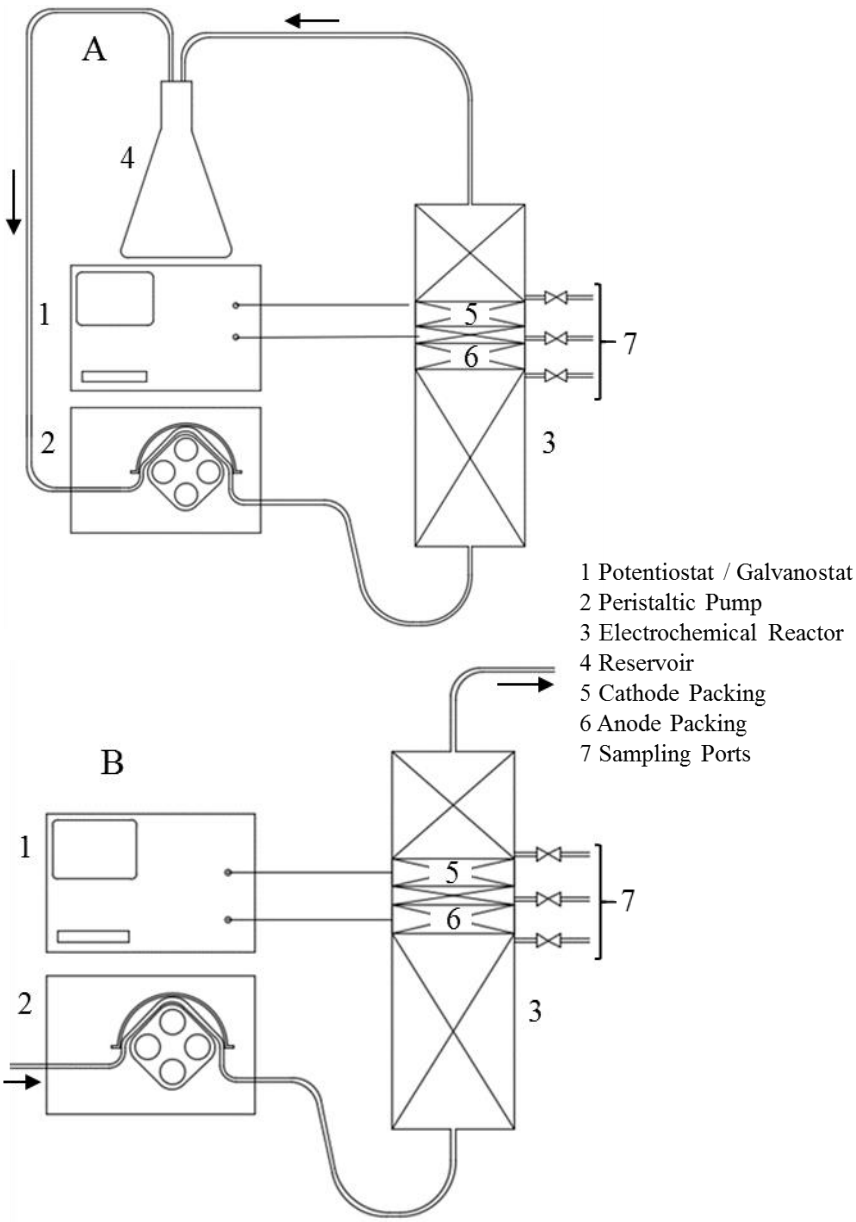

Figure 2. *Hydraulic scheme of the system in: batch recirculated mode (A), and continuous mode (B) configurations.*

2.2.4. Analyses

Inactivation of *M. aeruginosa* and *C. vulgaris* microalgae was monitored through the absorbance at λ = 680 nm (corresponding to the maximum absorbance of chlorophyll-*a*), with a Spectrophotometer (VARIAN-50). An example of typical absorption spectra with the chlorophyll-*a* peak at the corresponding wavelength is shown in *Figure 3*. Cell counting by an optical microscope at ×40 (Olympus) and Thoma chamber was also used as a comparison (see *Figure 27B*, Appendix (I)). There was a linear dependence between the algal concentration and the absorbance in all the performed experiments.

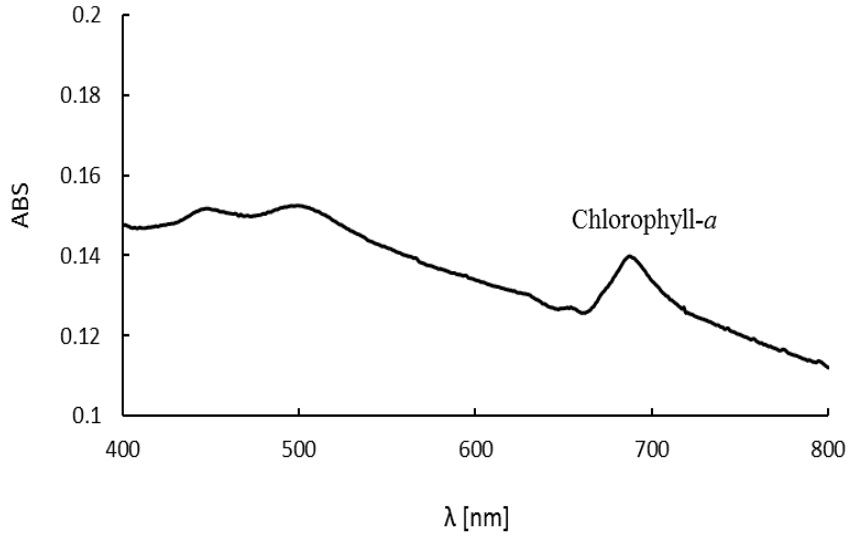

Figure 3. *Example of a typical algae chlorophyll-a pigment absorption spectra at 680 nm.*

The oxidants concentration, expressed as mg dm^{-3} of Cl_2, was measured using the N,N-diethyl-p-phenylenediamine (DPD) colorimetric method from samples filtered through a 0.45 µm filter (Whatman syringe filter). The DPD method provides a measure of the global concentration of the

oxidising species contained in the sample; ClO^-/HClO, Cl_2. The method is effective for active chlorine concentrations ranging from 0.05 to 2 mg dm^{-3}. Interference of chloride and nitrate ions was not reported up to a concentration of 1000 g m^{-3} (samples were diluted when necessary). Positive interferences are possible in presence of H_2O_2 and O_3 when DPD method is used: nevertheless, the reaction of H_2O_2 with DPD is slow and requires a peroxidase catalysed reaction, while ozone can quickly react with DPD even if its response is not stable. In order to differentiate among the different species, the actual content of hypochlorite was also derived from the direct UV analysis (ClO^- absorption peak at 292 nm), correcting the pH of the samples up to 11: appreciable peak in the UV spectra has been recorded at least when ClO^- concentration was greater than 2 mg dm^{-3}. The comparison between DPD and UV analyses indicated that the main compound was active chlorine.

An ion chromatograph was used to determine the concentrations of the ionic species (IC 761 Metrohm, Switzerland). The analytic conditions were the following: conductivity detector; ion exchange column (6.1006.430 Metrosep, Metrohm, Switzerland); 2 mM $NaHCO_3$/1.3 mM Na_2CO_3 as mobile phase; flow rate 1.5 cm^3 min^{-1}. The identification of the species was based on the retention times; the quantification was performed by external calibration. Ion chromatography allowed the direct measure of ClO_3^- and ClO_4^-, when present: since Cl^- and ClO^- have overlapping peaks, the analysis was repeated after the samples were treated with sodium sulphite in order to reduce hypochlorite to chloride. The concentration of Cl^- was obtained from the solution of the algebraic equations in which the unknowns are the chloride concentration and the scale factor from the peak area to the hypochlorite concentration [31].

Each sample was analysed three times, high repeatability was observed, with differences within 5% in all cases.

2.2.5. Mass transfer characterisation

As it is a very common practice in electrochemistry [46–48], the standard redox ferricyanide/ferrocyanide couple has been adopted to characterise the mass transport in the cell. The apparatus used for these studies was that showed in *Figure 2B*. The method is based on the reduction of ferricyanide to ferrocyanide ions allowing the convective-diffusion controlled limiting current density (i_L) to be measured over a range of flow rates of electrolyte. The limiting current densities were measured for $K_3Fe(CN)_6$ 1 mM reduction and in presence of an excess of $K_4Fe(CN)_6$ (0.1 M), in order to ensure that the anodic reaction never became the limiting process. The supporting electrolyte was 0.5 M Na_2CO_3.

The values of cathodic mass-transfer coefficient (k_m^c) at the relevant *Re* numbers were derived from equation (5) and are reported in *Table 2*:

$$k_m^c = \frac{i_L}{n_e \cdot F \cdot c_b} \qquad (5)$$

Table 2. *Values of the cathodic mass-transfer coefficients at the relevant Re values calculated with equation* (5).

Re	k_m^c x 10^5 [m s^{-1}]
10	0.88
20	1.09
30	1.19
40	1.33
60	1.43
80	1.59
120	1.79

The values of $k_m{}^c$ were then used to obtain a dimensionless mass-transfer correlation in the form, where the 0.33 power of the Schmidt number was assumed *a priori*.

$$Sh = p \cdot Re^q \cdot Sc^{0.33} \quad (6)$$

Figure 4 shows the fitting parameters values of q and p, which were obtained from the slope and from the intercept of the linear regression.

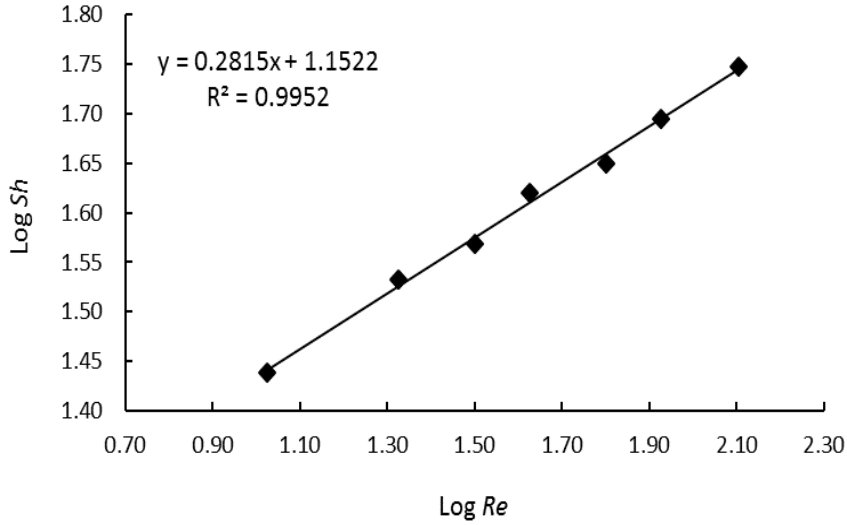

Figure 4. *Linear regression for the logarithm of Re versus logarithm of Sh dimensionless numbers.*

The values of p and q obtained are 1.15 and 0.28, respectively; these values are in agreement with those typical of laminar flow in fixed bed reactors with geometrical characteristics similar to the electrochemical cell adopted in this work.

The procedure description of the electrochemical technique employed for the mass-transfer characterisation can be found in Appendix (II).

2.2.6. Hydrodynamic characterisation

The hydrodynamic characterisation of the cell was performed by pulse response tests using the experimental scheme described in *Figure 5*.

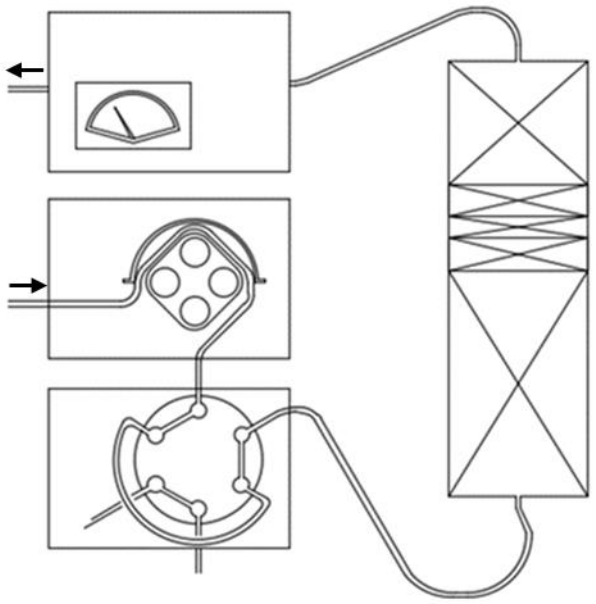

Figure 5. *Experimental apparatus used for pulse response experiments.*

A sharp pulse of inert tracer (3 M KCl) was injected upstream the system through a six-port valve at different inlet flow rates, while a conductivity detector located at the outlet recorded the concentration of the tracer in outlet stream. The response of the detector was the residence time distribution (RTD). The analysis of the experimental momentum analysis was done calculating the following parameters:

Exit age distribution *E(t)*

$$E(t) = \frac{C(t)}{\int_0^\infty C(t) \cdot dt} \qquad (7)$$

Mean residence time t_m

$$t_m = \frac{\int_0^\infty t \cdot C(t) \cdot dt}{\int_0^\infty C(t) \cdot dt} = \int_0^\infty t \cdot E(t) \cdot dt \quad (8)$$

Variance σ^2

$$\sigma^2 = \frac{\int_0^\infty (t-t_m)^2 \cdot C(t) \cdot dt}{\int_0^\infty C(t) \cdot dt} = \int_0^\infty (t-t_m)^2 \cdot E(t) \cdot dt \quad (9)$$

The RT data experimentally obtained for different *Re* values are represented in *Figure 6*.

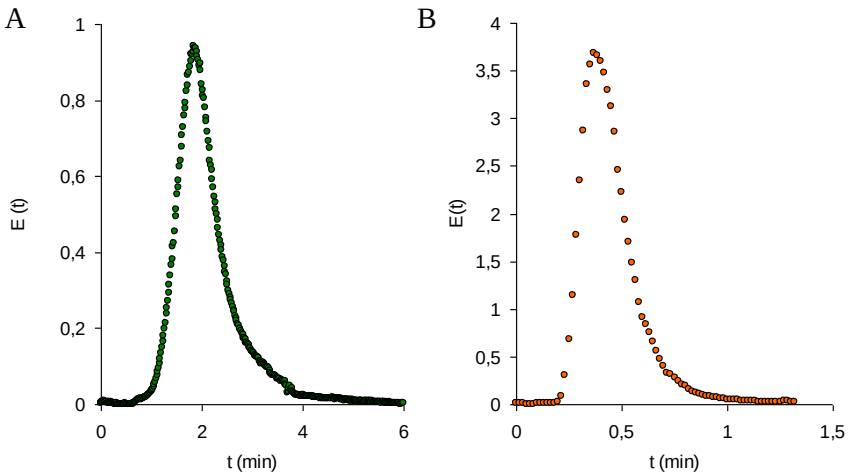

Figure 6. *Experimental E(t) curves obtained at different Re values. Re = 40 (A) and Re = 160 (B).*

A well-shaped single peak was always obtained with a relatively long tail; the shape of the curves depended on the flow rates, and clearly indicated that the system was under non-ideal flow conditions since the existence of

possible dispersion phenomena, dead or stagnant zones, bypass flows, exchanges between them and recirculation zones [39].

The values of mean residence time and variance for each flow rate are represented in *Table 3*.

Table 3. *Values of mean residence time and variance of the peaks calculated with equations (8) and (9) at different Re values.*

Re	t_m [min]	σ^2 [min^2]
10	22.3	19
40	4.2	2.1
160	2.8	0.45

From these values the Peclet number was calculated using the correlation for closed-closed systems:

$$\frac{\sigma^2}{t_m^2} = \frac{2}{Pe} - \frac{2}{Pe^2} \cdot (1 - e^{-Pe}) \qquad (10)$$

This first estimated *Pe* value was then used to obtain values of axial dispersion coefficient (*D*) derived from the *Pe* dimensionless number:

$$Pe = \frac{v \cdot d}{D} \qquad (11)$$

The values of the axial dispersion coefficient obtained were of 0.5×10^{-5} m^2 s^{-1} (*Re* = 160), 0.3×10^{-5} m^2 s^{-1} (*Re* = 40) and 0.1×10^{-5} m^2 s^{-1} (*Re* = 10).

2.3. Results and discussion I

2.3. Results and discussion I

2.3.1. Batch recirculated experiments with BDD anode

Electrolysis experiments for *C. vulgaris* and *M. aeruginosa* inactivation, in the presence and in the absence of chloride ions in the inlet stream, were carried out in batch recirculated mode employing BDD anode, with the system configured as in *Figure 2A* (see 2.2.2).

2.3.1.1. Electrolysis of *C. vulgaris* algae

Figure 7 shows the semi-logarithmic trend with time of the normalised chlorophyll-*a* removal during chloride-free electrolyte-batch recirculated electrolyses under several applied current densities and flow rates.

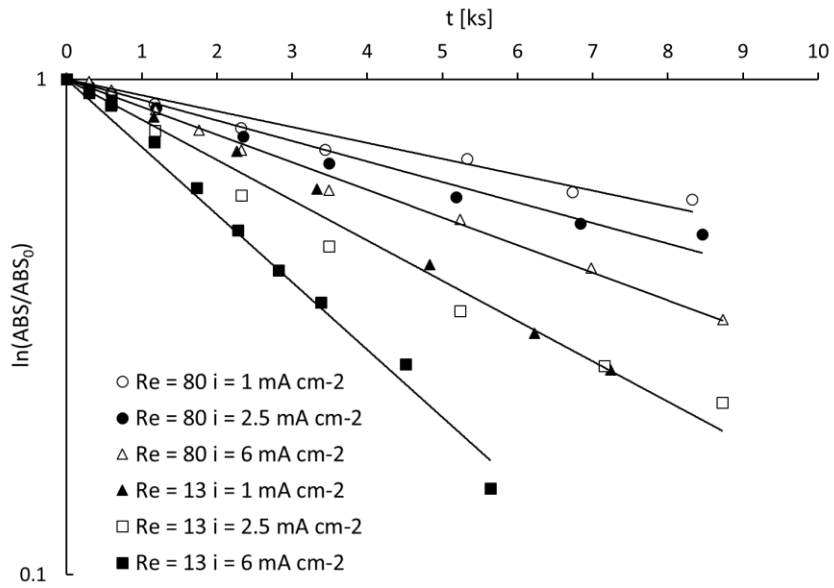

Figure 7. *The semi-logarithmic trend with time of the normalised removal of chlorophyll-a during batch recirculated electrolyses under different experimental conditions in a chloride-free electrolyte when BDD electrode was employed.*

The statistics of the linear regression of data are reported in *Table 4*, where *F* is the ratio between-groups variance divided by within-groups variance. *P* values indicate the statistical significance: if the computed *P-value* is <0.05, then significant relationships exist.

Table 4. *Values of the apparent kinetic constant (k_{app}) in the relevant experimental conditions for the linear regression statistics for the semi-logarithm of the C. vulgaris chlorophyll-a concentration ln(C/C_0) versus time.*

			Regression Statistics			Regression line	
Re	i [A m^{-2}]	ΔE_{CELL} [V]	F	P	R^2	k_{app} x 10^4 (±5%) [s^{-1}]	standard error
80	10	7.5	513.24	8.3E-08	0.992	0.73	1.96E-04
80	25	12.0	654.62	2.3E-07	0.995	0.95	2.24E-04
80	60	21.7	3358.49	8.7E-12	0.999	1.28	1.33E-04
13	10	7.4	1501.11	2.0E-08	0.998	1.82	2.81E-04
13	25	11.9	813.88	1.2E-07	0.996	1.87	3.94E-04
13	60	20.4	1900.49	8.5E-11	0.998	3.13	4.32E-04

Data suggest that the removal rate can be interpreted by a pseudo-first order kinetics, where the apparent kinetic constant (k_{app}), calculated from the slopes of curves in *Figure 7*, depends on both flow rate and applied current density. As reported, at a fixed current density the increase of *Re* values from 13 to 80 caused a twofold decrease in k_{app}.

On the other hand, *Figure 7* and *Table 4* show that for a set value of *Re* the applied current density has a significant effect on the removal process. In particular, when the current density passes from 25 to 60 A m^{-2}, an increase of 33% in k_{app} is observed at *Re* = 80, whilst the k_{app} increases by 65% at the lowest *Re* value. These results can be explained by considering the mechanism of microalgae inactivation and the geometry of the adopted system. As it will be explained extensively throughout this thesis, under the operations here used, the algal inactivation is mainly attributed to the disinfection actions of oxidants electrogenerated by the DE system [49,50]

and confirmed by other previous papers [31,38]. Moreover, the applied potential gradient can promote the formation of transient or permanent pores in the membrane wall of the algal cells, thus facilitating the attack of the electrogenerated oxidising species inside the cell [28,51].

Taking into account the geometry of the system, three different zones can be identified: the anodic and the cathodic reaction zones, which correspond to the two electrode areas in the DE system; and the bulk zone, which comprehends reservoir, tubing and inert packing of the DE system.

The chemical and electrochemical reactions occurring in the BDD anode zone during the electrolysis of water containing sulfates, lead to the formation of different oxidants, according to the reactions (r1–r8) defined in *Table 1*.

The oxygenated radicals desorbed from the BDD electrode surface (r1–r3) [49] react with water either in proximity of the anode or in the bulk zone, to generate oxygen (r4, r5) and other reactive oxygen species (ROS) (r6, r7) [30,52]. In addition, peroxydisulfates can also be generated (r8) [33,34]. In the cathode zone, along with the hydrogen evolution reaction (r21), the reduction of oxidants (r22, r23) may occur [50].

The presence of oxidants in the bulk zone during the batch recirculated-galvanostatic electrolysis of water in the presence and absence of *C. vulgaris* was monitored. The detection of oxidants with the DPD colorimetric method used was possible, however, only for current densities higher than 40 A m^{-2} and *Re* equal to 13. *Figure 8* compares the trend of the concentration of oxidising species as a function of time for runs carried out at *Re* = 13 and i = 40 A m^{-2}.

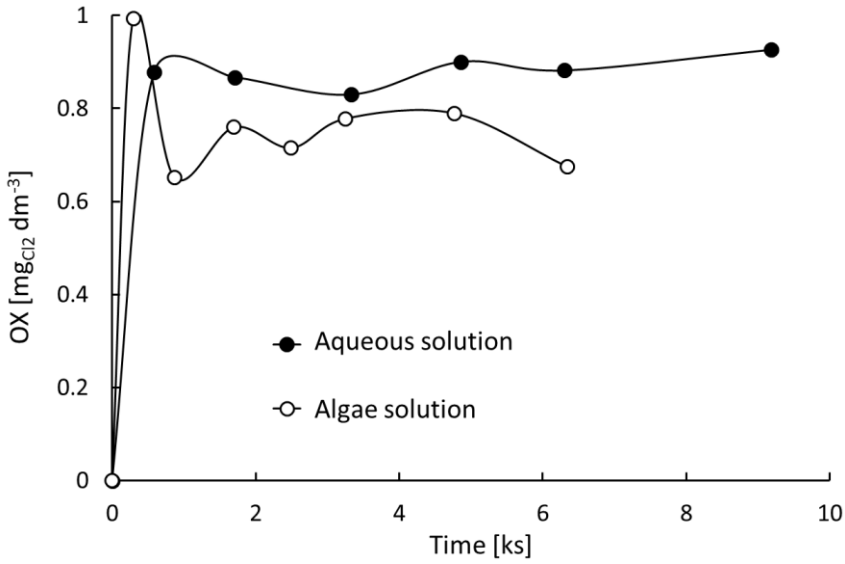

Figure 8. *Trend with time of oxidants measured by DPD method, as mg dm^{-3} of equivalent Cl_2, for batch recirculating electrolysis at Re = 13 and i = 40 A m^{-2} in the presence and absence of C. vulgaris algae when BDD anode was used.*

A pseudo-steady value in the concentration of oxidants was observed after few minutes of electrolysis. This pseudo-steady state is a result of the balance between anodic generation, cathodic reduction and spontaneous decay in the bulk solution (r19, r20). The concentration of oxidants is, however, very low, thus indicating that most of the oxidants generated are reduced in the cathode zone [53]. Since the difference in oxidant concentration in the presence and absence of algae was only marginal, we assume that the reaction of oxidants with *C. vulgaris* (i.e. the contribution of bulk disinfection to the removal process) is negligible. Different results were obtained in the following case investigated, under similar conditions but in the presence of 100 mg dm^{-3} of chlorides (see 2.3.1.2), nearly a threefold increase in the oxidants concentration was reached. Under these conditions the reaction with bulk oxidants, mainly constituted by active chlorine species, was the main responsible for the inactivation of *M. aeruginosa* algae [49].

In a chloride-free electrolyte, the inactivation of microalgae is likely to occur in the anode zone, and it is due to a synergistic effect caused by the applied electric field and the very high concentration of oxidants in that area. As such, the value of k_{app} mainly depends on the electric potential, the concentration of oxidants, as well as on the hydraulic residence time in the cell.

Both the potential and concentration of oxidants within the anodic packed bed are controlled by the current density. Therefore, high values of current density correspond to high values of specific inactivation rate k_{app}, which increases with the residence time within the anodic zone, and therefore is inversely proportional to *Re*, as reported in *Table 4*.

Figure 9 reports the amount of electrical energy, E_r, required to remove 50% (*Figure 9A*) and 75% (*Figure 9B*) of the initial concentration of *C. vulgaris*. E_r was calculated by changing the value of a given removal (R) (between 0–1) in equation (12) and by using the values of cell potentials reported in *Table 4* under different conditions of flow rate and current density.

$$E_r = \frac{I \cdot \Delta E_{CELL} \cdot t}{V} = -\frac{I \cdot \Delta E_{CELL}}{V} \cdot \frac{\log(1-R)}{k_{app}} \qquad (12)$$

As it can be expected, the energy requirement is lower for *Re* = 13, where k_{app} reaches its maximum value, and at i = 10 and 25 A m^{-2}, characterised by relatively low cell potentials.

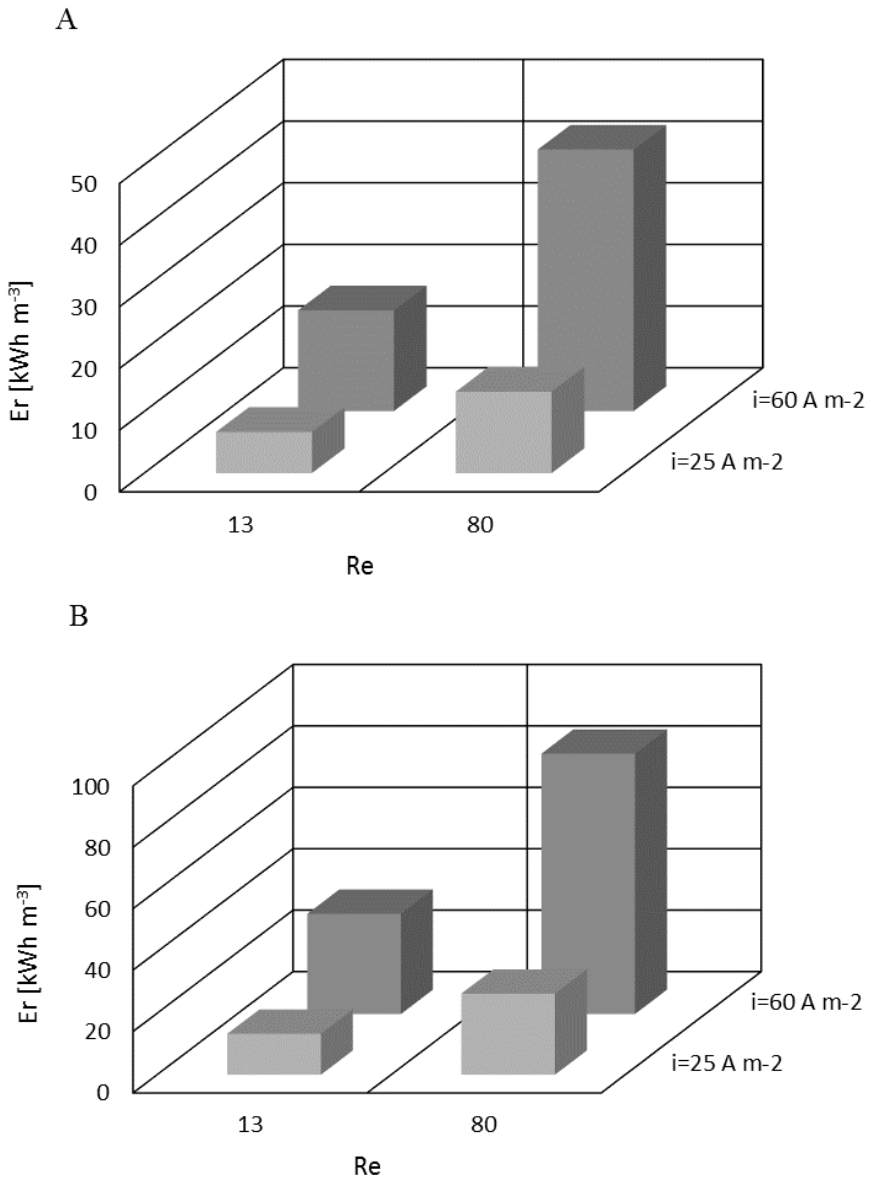

Figure 9. *Electrical energy required by the DE cell for R = 0.5 (A) and R = 0.75 (B) inactivation of the initial concentration (15 x 10^6 cells ml^{-1}) of C. vulgaris.*

2.3.1.2. Electrolysis of *M. aeruginosa* algae

Figure 10 shows the trend with time of the chlorophyll-*a* removal, in a solution containing chloride ions, during electrolysis runs in batch recirculated mode under different working conditions.

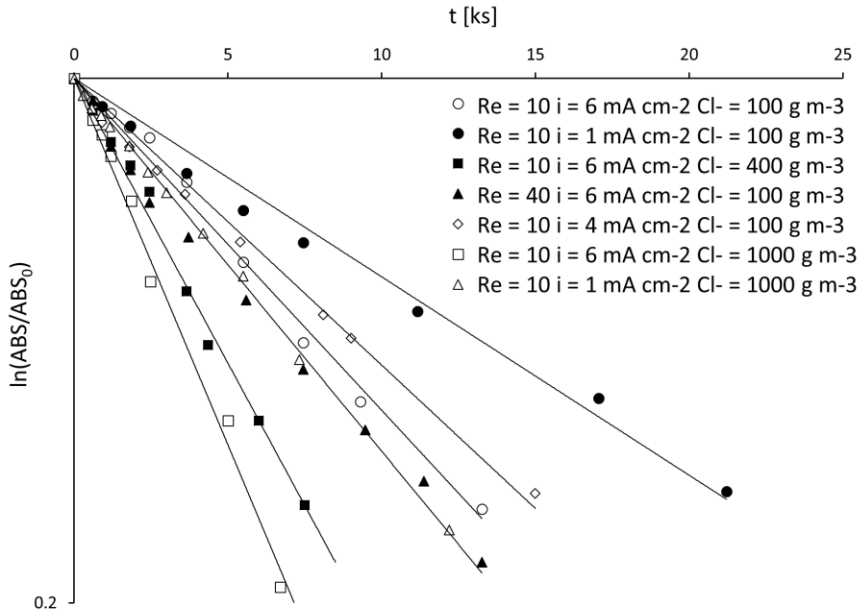

Figure 10. *The semi-logarithmic trend with time of the normalised removal of chlorophyll-a during batch recirculated electrolyses under different experimental conditions in a chloride electrolyte when BDD electrode was employed.*

A removal of about 80% has been reached in all the analysed cases, after different electrolysis times, which depended on the experimental conditions. At *Re* = 10 and i = 60 A m^{-2} in solution containing 1000 g m^{-3} of chloride ions, the maximum removal was reached after 6 ks of electrolysis, whereas more than 20 ks were necessary under the weakest condition. The removal rates can be compared with those obtained during electrolysis of *C. vulgaris* with BDD anodes [26], although the reactor used

was a filter-press, runs were carried out under similar conditions of current density and chloride concentrations. Moreover, k_{app} can be also compared with those obtained in a chloride-free electrolyte (*Table 4*). Hence, the removal rates with *M. aeruginosa* are considerably lower than those with *C. vulgaris*, confirming the high resistance of these microorganisms [54–56].

Table 5 shows the linear regression statistics for the logarithm of the *M. aeruginosa* chlorophyll-*a* concentration $\ln(C/C_0)$ versus time, where *F* and *P* were previously defined in 2.3.1.1.

Table 5. *Values of the apparent kinetic constant (k_{app}) in the relevant experimental conditions for the linear regression statistics for the semi-logarithm of the M. aeruginosa chlorophyll-a concentration $\ln(C/C_0)$ versus time.*

				Regression Statistics			Regression line	
Re	i [A m^{-2}]	ΔE_{CELL} [V]	Cl^- [g m^{-3}]	F	P	R^2	k_{app} x 10^4 (±5%) [s^{-1}]	standard error
10	10	13.1	100	1304.20	3.0E-08	0.99	0.61	1.69E-03
10	40	18.0	100	1845.52	1.1E-08	0.98	0.92	2.05E-03
10	60	20.5	100	2142.72	5.7E-10	0.99	1.02	2.20E-03
40	60	25.0	100	1829.15	9.8E-11	0.99	1.14	2.68E-03
10	10	7.9	1000	12030.77	2.2E-15	0.99	1.14	1.04E-03
10	60	17.2	400	2229.72	6.0E-09	0.97	1.75	3.70E-03
10	60	16.1	1000	1519.91	2.1E-07	0.97	2.21	5.77E-03

A positive effect of the applied current density on the removal rate can be observed. In particular, increasing the current density from 10 to 40 A m^{-2}, k_{app} increases by 50%. Lower, but still appreciable effect of flow rate was obtained, with an increase of 10% in k_{app}, passing from *Re* = 10 to *Re* = 40, current density being the same. The effect of chloride ions concentration on the process appears as the most relevant under the experimental conditions adopted. Anyway, the results clearly indicate that the inactivation of algae is influenced by current density, hydrodynamics and chloride concentration.

Even though the inactivation of microorganisms is still not well understood, different mechanisms can be identified, which may be responsible for cell inactivation: in the bulk of the solution, the disinfection by electrogenerated oxidants has been proved as the main mechanism [31,38,50]. Some authors also reported a possible effect of the potential gradient on the cell membrane: usually, this effect is significant at high electric field (namely higher than 10^3 V cm^{-1}). However, it can also be effective at values in the order of tens V per square cm, using electrodes with pore size 4 orders of magnitude larger than bacteria [23].

The concentration of oxidants depends on the different and complex phenomena that typically occur during electrolysis with BDD anodes: the prevalence of one mechanism depends on the operative conditions and on the nature of microorganisms. As an example, the removal of *Escherichia coli* from chloride-free solutions, was attributed to electric field [23], but also to oxygenated radicals near the anode surface [53], or to bulk oxidants disinfection [52]. In the presence of chlorides, the higher amount of bulk oxidants, mainly chlorinated, increased the relevance of bulk disinfection in *E. coli* removal [39]. Microalgae showed a higher resistance during electrolysis: the inactivation of *C. vulgaris* in a filter-press cell with BDD was only possible in the presence of chlorides, under the conditions of strong generation of oxidants, high current densities and chloride concentrations [26].

Figure 11 shows the trend with time of bulk oxidants concentration, as equivalent Cl_2 measured by DPD method, during batch recirculated electrolysis of solutions containing *M. aeruginosa*.

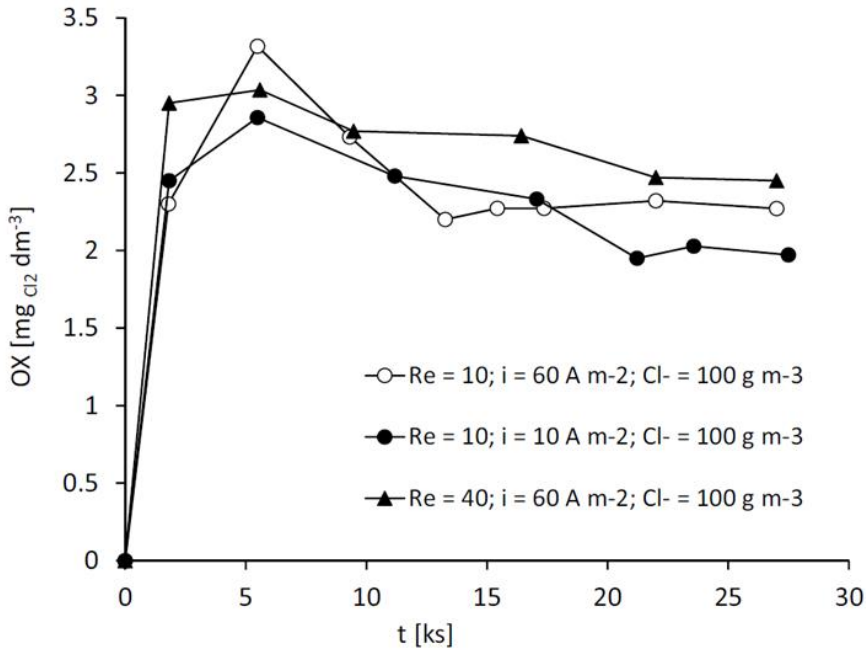

Figure 11. *Trend with time of oxidants measured by DPD method, as mg dm^{-3} of equivalent Cl_2, for batch recirculated electrolyses under different experimental conditions when BDD anode was tested.*

As can be observed, the values are relatively low if compared with those obtained in electrolyses of chloride solutions [31,39,42], indicating a consumption of oxidants by microorganisms. Moreover, data follow the behaviour of a reaction intermediate, with a maximum and a pseudo steady state; comparing *Table 5* and *Figure 11*, we can observe that the highest values of oxidants are obtained under the conditions at which k_{app} of *M. aeruginosa* reached the maximum values. The results suggest that the reaction with bulk oxidants is the main mechanism of the inactivation process of *M. aeruginosa* by electrolysis with BDD anodes, confirming the results obtained with *C. vulgaris* in the previous study (see 2.3.1.1) and affirmed also with those achieved in a filter-press cell [26].

An increase in the current density increases the amount of radicals electrogenerated, (reactions (r1–r3) in *Table 1*), which in turn increases the production of bulk oxidants (r6–r8) generated by chemical reactions involving radical species. Active chlorine arises from chloride oxidation by direct electron transfer (r9), so that it is directly related to the applied current density. Being oxidation of chloride kinetically favoured at BDD, the amount of current for active chlorine production mainly depends on the Cl^- concentration.

Moreover, the strong influence of Cl^- ions concentration on the oxidants generation suggests that the bulk oxidants are mainly constituted by active chlorine species, as already observed [26], even if the solution contains high amount of sulfates. The slow increase in the bulk oxidants with *Re* may be due to the decrease of cathodic reduction of active chlorine, which is a fast electrochemical reaction with a diffusion-controlled kinetics at the low concentration of active chlorine detected.

As the energy consumption is concerned, *Figure 12* shows the amount of E_r supplied to inactivate the 80% of the initial algal biomass for data obtained at *Re* = 10 under different concentration of chlorides and current densities; values of cell potentials under the different conditions are reported in *Table 5*. The parameter was calculated as $E_r = a \cdot i \cdot \Delta E_{CELL} \cdot t_{80}$, where t_{80} is the time to reach 80% of inactivation.

According to the trend of the inactivation rates, the minimum energy consumption was obtained with the highest concentration of chlorides. The values are higher than those calculated for inactivation of *C. vulgaris*, which were in the range 2.5–3 kWh m^{-3} under similar conditions of current densities, cell potentials and initial concentration of microalgae [26]. This furtherly confirms the higher resistance of *M. aeruginosa* to the electrochemical treatment, which leads to a lower inactivation rate, and then to low current yield, so increasing the energy required to achieve the same inactivation yield.

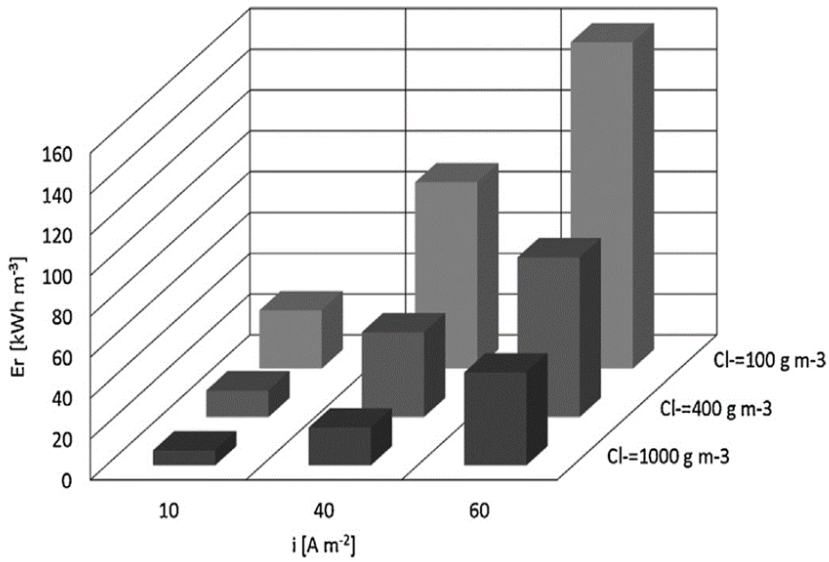

Figure 12. *Energy requirements of the process for the inactivation of M. aeruginosa for electrolyses in batch recirculated mode at Re = 10 under different current densities and inlet Cl^- ions concentrations when BDD anode was employed.*

A direct comparison with literature values is not straightforward, due to the different conditions: Xu et al. [24] obtained values of 4–6 kWh m^{-3} for 80% inhibition of *M. aeruginosa* growth, by electrolysis with Ti/RuO_2 anodes at current densities of 20–40 A m^{-2}. Liang et al. [25] used Ti/RuO_2 for electrolysis of *M. aeruginosa* in a recirculated system: the authors did not give direct information on energy consumption, however one can calculate values of about 10–15 kWh m^{-3} at 100 A m^{-2}. Moreover, we can compare our values with other electrical energy based treatments, such as electrocoagulation processes, for which the literature reports values in the range from 0.4 to 18 kWh m^{-3} [18,19].

2.3.2. Continuous experiments

Electrolysis experiments for *M. aeruginosa* inactivation were also carried out in continuous mode employing both DSA and BDD anodes, with the system configured as in *Figure 2B* (see 2.2.2).

2.3.2.1. Electrolysis with DSA anode

Figure 13 shows the percentage of the chlorophyll-*a* removal, as a function of the ratio between the electrolysis time and the hydraulic residence time, obtained under different operative conditions when DSA anode was employed.

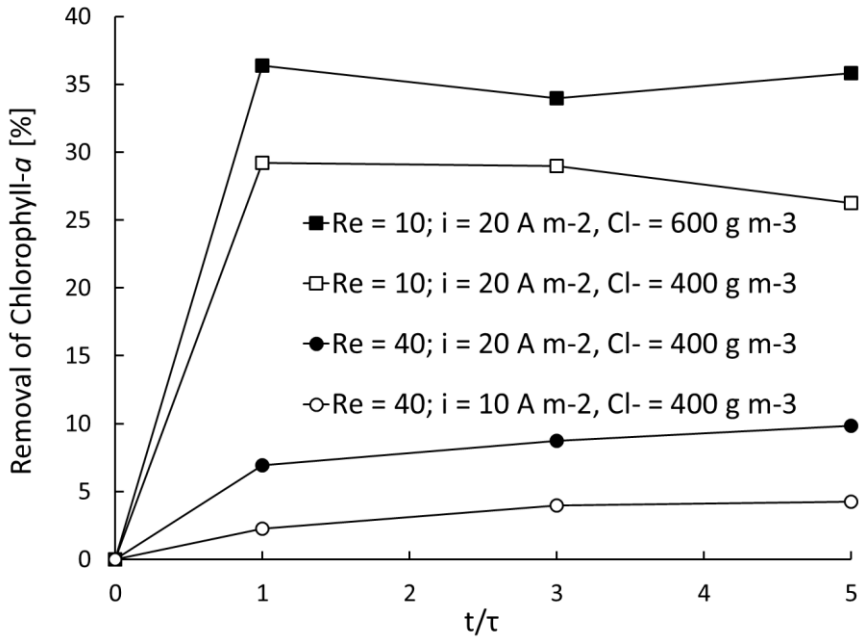

Figure 13. *Trend of the chlorophyll-a removal as a function of the ratio between electrolysis time and residence time obtained under different operative conditions.*

For all the runs, it can be noticed that the removal quantity of chlorophyll-*a* increases significantly up to 1 hydraulic residence time, and at this time the system reaches the steady state.

By operating at *Re* = 40, *i* = 10 A m^{-2} and Cl^- = 400 g m^{-3}, the removal efficiency of the chlorophyll-*a* amounted to 4.24%. On the other hand, working at 20 A m^{-2} and maintaining constant the other parameters, the algae removal reached the 9.83%. The highest removal of chlorophyll-*a* (33.95%) was obtained when an initial concentration of 600 g m^{-3} of chloride ions were used, operating with the lowest flow rate and at the highest current density. Comparing the experiments performed at 400 g m^{-3} with those at 600 g m^{-3}, it is possible to observe that the more the amounts of Cl^- ions present, the more the chlorophyll-*a* removal.

As the effect of the hydrodynamic of the reactor is concerned, a decrease in the removal of the normalised absorbance can be observed as the hydraulic residence time decreases. In particular, the real flow inside the treatment unit is of great concern when a process for microorganisms is considered; the presence of the dispersion phenomena, dead or stagnant zones and bypass flows may lead to an inaccurate estimation of residence times required for an effective process [39].

This behaviour may be interpreted considering the different phenomena occurring during the electrolysis of water with DSA, and the possible mechanisms responsible for algae inactivation (see 2.1). It is worth highlighting that in a previous work, appreciable amounts of other chlorinated compounds were not detected under conditions similar to those adopted in this work [26].

The ability of active chlorine to attack the proteins of the cell membrane, the protoplasm and the nucleus of the cell is well documented [52], and the role of the active chlorine species was also investigated for algae removal processes [17].

The behaviour of the system was investigated first with solutions only containing the growing medium, to which different amounts of chlorides were added. Electrogenerated bulk oxidants concentration were measured

in the outlet stream when the process achieved the steady state, as equivalent Cl_2 measured by DPD method. *Figure 14* shows the concentration of active chlorine formed in the outlet stream as a function of the flow rate and the applied current density with two different initial concentration of chlorides ions: 200 g m^{-3} (*Figure 14A*) and 400 g m^{-3} (*Figure 14B*).

The generation of active chlorine increased with the current density and decreased with the flow rate. Under the conditions adopted in this work, the currents of migration and diffusion of chlorides are of the same order of magnitude, and the kinetic of chloride oxidation is under mixed current/mass transfer control [44]. The effect of current density and inlet concentration of Cl^- ions observed is expected, while the flow rate may differently affect the process.

At low flow rate, the residence time of the electrolyte inside the cell is relatively high in both the electrode compartments. In the anode packing high contact times favour the formation of active chlorine.

At the cathode we have to consider the negative effect due to the increased residence time for active chlorine reduction, but also the positive effect of low mass transfer rate, which is the controlling step of the cathodic reduction of active chlorine.

High values of flow rate lead to low contact times, which may reduce the formation of active chlorine, but also balance the increase of the specific rate of active chlorine reduction.

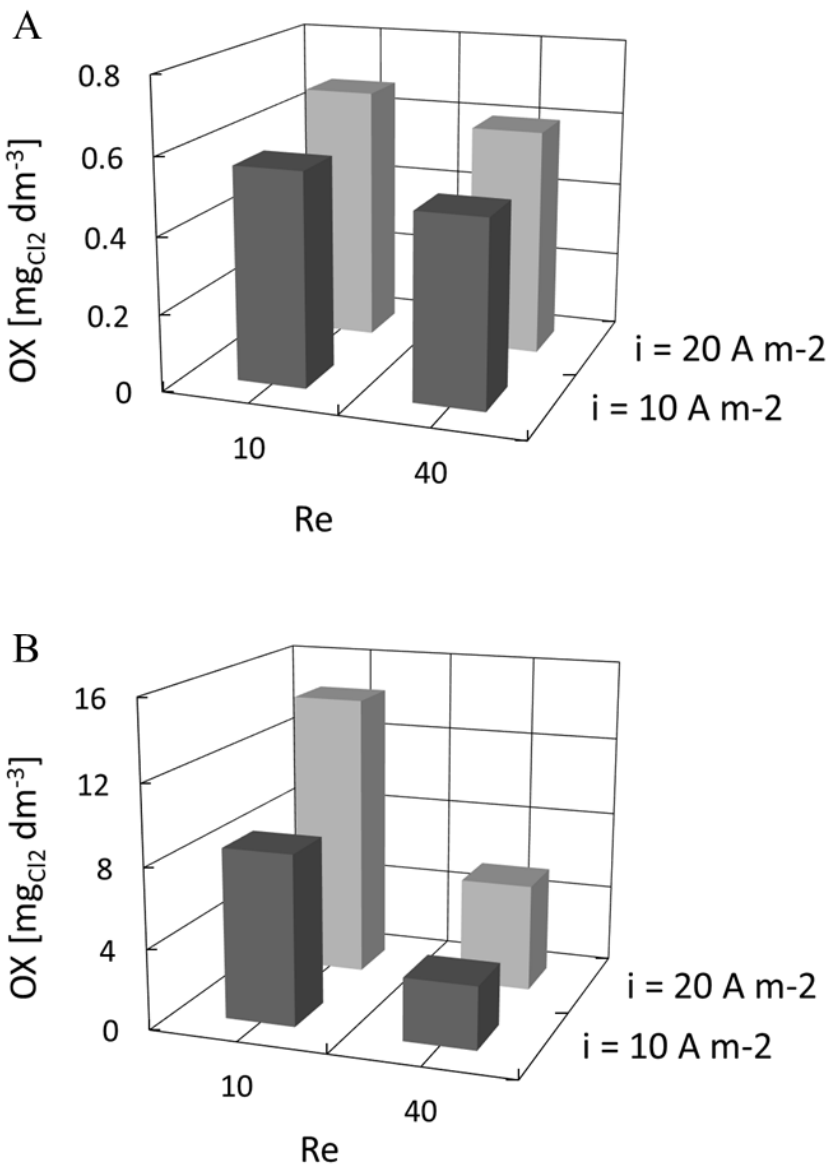

Figure 14. *Steady state concentrations of electrogenerated oxidants in the outlet of the reactor measured by DPD method, as mg dm^{-3} of equivalent Cl_2. Data obtained from continuous electrolysis under different flow conditions, applied current densities, and with 200 (A) and 400 g m^{-3} (B) of chloride ions when DSA anode was tested.*

Active chlorine formation was also investigated with *M. aeruginosa* in the inlet of the reactor. *Figure 15* shows the comparison of active chlorine concentrations measured in the outlet stream from continuous electrolysis in the presence and in the absence of *M. aeruginosa* algae. The concentration of chloride ions in the inlet stream was 400 or 600 g m^{-3}. The experiments were performed with a current density of 20 A m^{-2} at *Re* = 10. It is worth observing that only under these conditions of relatively high current density and high chloride ions concentration the active chlorine was present in detectable amount.

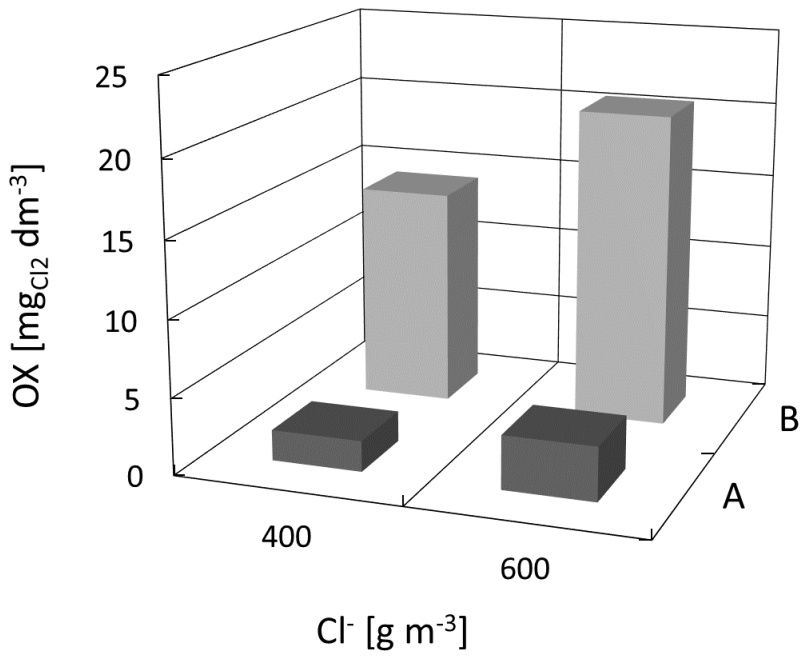

Figure 15. *Steady state concentrations of electrogenerated oxidants in the outlet of the reactor measured by DPD method, as mg dm^{-3} of equivalent Cl_2. Data obtained from continuous electrolysis under different Cl^- concentrations, current density of 20 A m^{-2}, and Re = 10 in the presence (A) and absence (B) of M. aeruginosa in the inlet stream when DSA anode was tested.*

Active chlorine concentrations below 2 mg dm^{-3} were obtained with 400 g m^{-3} of chloride ions, while higher values were obtained with 600 g m^{-3}, but in any case, the presence of algae strongly reduced the active chlorine concentration in the outlet stream. This result leads to the conclusion that the bulk phenomena are prevalent in the algae removal process, under the conditions adopted in this work.

The active chlorine formed at DSA anode may react with the high organic load originated by the presence of microalgae, so that the difference in oxidants concentration detected with and without algae, may be attributed to the consumption of the oxidising species by *M. aeruginosa*. This may be confirmed by the trend of removal efficiency with the flow rates: passing from *Re* = 10 to *Re* = 40, chloride ions concentration and current density being the same, the removal efficiency resulted reduced by 60%.

2.3.2.2. Electrolysis with BDD anode

In the present case, the behaviour of the system without algae has been studied first. A mathematical model was implemented to simulate the behaviour of the system, based on the following assumptions:

- Cl^- and SO_4^- were not modelled since appreciable variation in the concentration of inorganic species between inlet and outlet was not detected because of the low contact times.
- The long-life (bulk) oxidants were considered as total oxidants (OX), which include active chlorine and other long-life oxidants, generated by DE (r9) or by a mechanism mediated by radicals electrogenerated (r6–r8, r12). The formation of OX was modelled through the sum of the currents related to reactions (r6–r9, r12).
- Two mechanisms for OX consumption were taken into account: the cathodic reduction, which was assumed a mass transfer controlled reaction, and the chemical decay in the bulk (r19, r20), which was modelled by a first order law.
- The occurrence of products of active chlorine oxidation, other than chlorates was neglected. Two mechanisms for the generation of chlorates were considered: the pseudo-surface reaction via oxygen radicals (r14, r17) and the chemical decay of bulk oxidants (r19, r20).

The first was modelled through the corresponding current, the second through a first order law. The concentration profiles along the reactor calculated by the model were compared with the experimental values obtained at the relevant experimental conditions.

The model equations are reported in the Appendix (III) along with the boundary conditions and the details of the model solution.

Table 6 summarises the values of model parameters and experimental conditions. The current fractions (ε_{OX} and ε_{ClO3-}) were the only adjustable parameters of the model, and were calculated through sensitivity analysis from the concentrations of the different species. Each value was obtained by a single set of experimental data.

Table 6. *Parameters used in the model (equations (22)–(25)).*

Re	*i* [A m^{-2}]	Cl^- [g m^{-3}]	k_m^c x 10^5 [m s^{-1}]	ε_{OX}	ε_{ClO3-}
10	25	100	0.88	0.0135	0.003
10	25	400	0.88	0.039	0.005
10	25	600	0.88	0.068	0.01
40	12	100	1.33	0.0135	0.003
40	25	600	1.33	0.068	0.01
160	25	100	2.03	0.0135	0.003

The comparisons between experimental and model predicted data in terms of concentration profiles of oxidants and chlorates at steady state are reported in the following figures. *Figure 16* shows data related to

electrolyses of BG 11 without *M. aeruginosa* with an inlet concentration of 100 g m^{-3} of chlorides, and different flow rates and current densities.

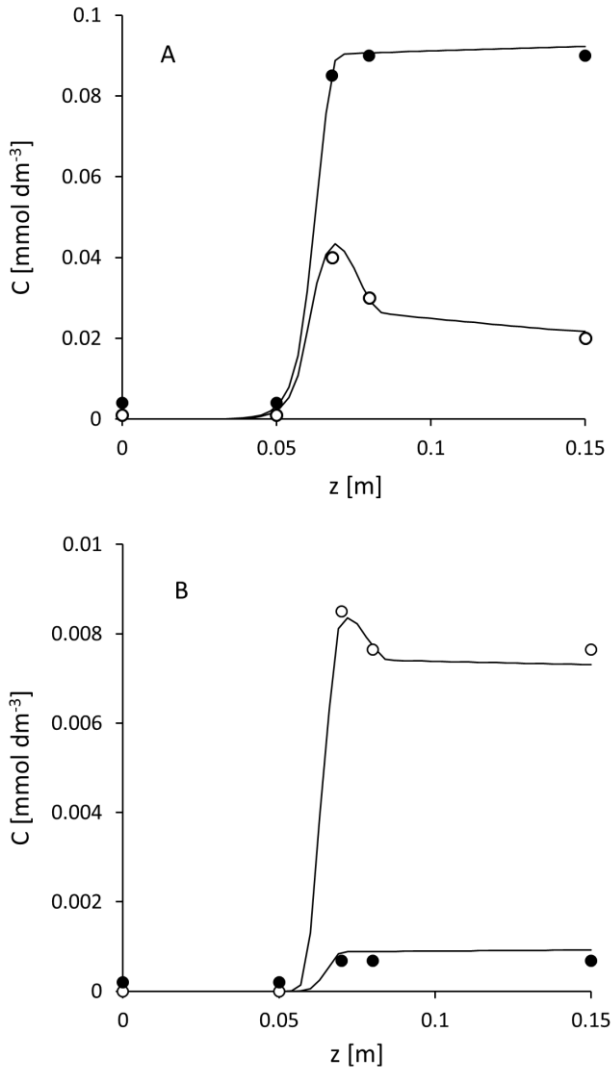

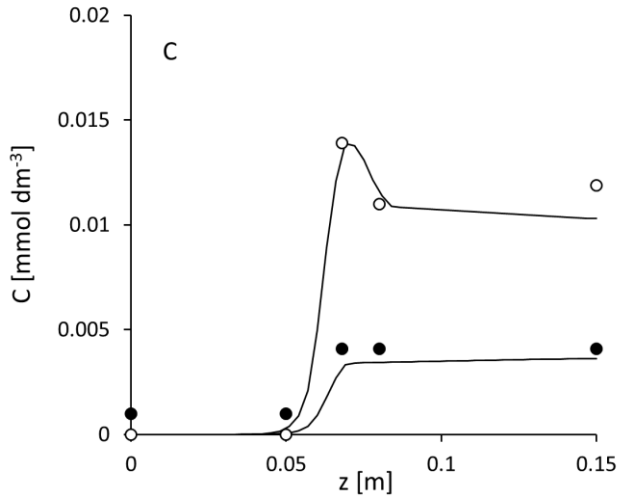

Figure 16. *Comparison between experimental (symbols) and model predicted (lines) concentration profiles of oxidants (empty symbols) and chlorates (full symbols) from continuous experiments at the steady state for solutions in the absence of M. aeruginosa with initial chloride concentration of 100 g* m^{-3} *under different flow conditions and current densities when BDD anode was employed A: Re = 10, i = 25 A* m^{-2}*; B: Re = 160, i = 25 A* m^{-2}*, and C: Re = 40, i = 12.5 A* m^{-2}*.*

An increase in the oxidants and chlorates concentration with the current density can be observed, while the increase in the flow rate causes a decrease of the same compounds. The trend with the current density was expected, since the faradaic yield for oxidants generation virtually depends on the inlet concentration of inorganic precursors [39], such as chlorides and sulfates. The effect of flow rate is less obvious: in the anode packing, the oxidation of chlorides to active chlorine is favoured by high values of τ (i.e. low *Re*). In the cathode packing, the main reaction is the active chlorine reduction, which is favoured by high residence time, but not by low mass transfer rates, both conditions occurring with low *Re*. The formation of chlorates is due to pseudo-surface and bulk reactions, both dependent on the hydraulic residence time, so that high *Re* dramatically decreases the concentration of chlorates in the outlet stream.

As the effect of chlorides is concerned, *Figure 17* describes the trend of data related to electrolysis without *M. aeruginosa* at i = 25 A m^{-2} under different flow conditions and inlet Cl^- ions concentration.

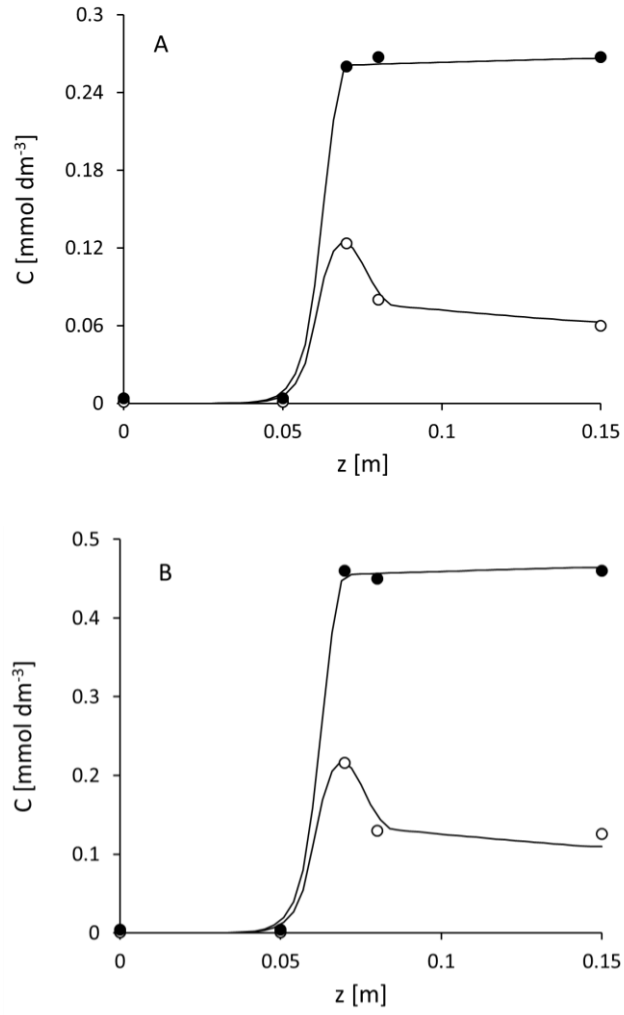

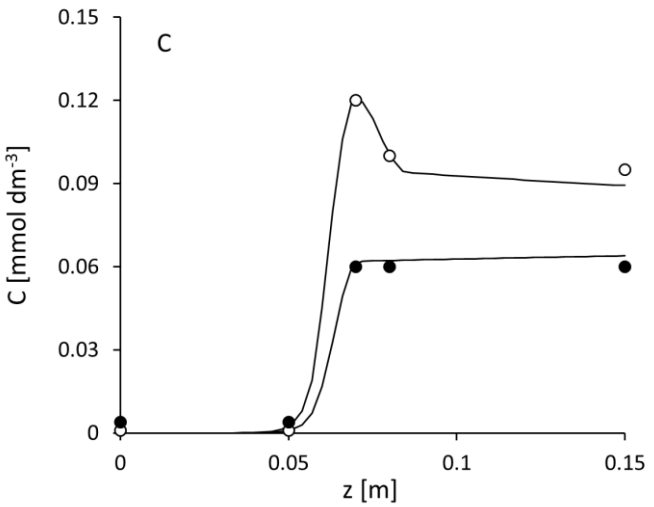

Figure 17. *Comparison between experimental (symbols) and model predicted (lines) concentration profiles of oxidants (empty symbols) and chlorates (full symbols) from continuous experiments at the steady state for data obtained at i = 25 A m^{-2} under different flow conditions and inlet Cl^- ions concentration in the absence of M. aeruginosa when BDD electrode was employed. A: Re = 10, Cl^- = 400 g m^{-3}; B: Re = 10, Cl^- = 600 g m^{-3}; and C: Re = 40, Cl^- = 600 g m^{-3}.*

As can be seen, the higher the Cl^- concentration in the inlet stream, the higher the concentration of oxidants in the outlet stream, the other operative conditions being the same. Moreover, similar effect can also be observed for the concentration of chlorates, which confirms the reactions involving chlorides as the most important processes.

Concentrations of chlorates in the outlet were generally higher than those obtained at DSA anodes with the same system and under similar conditions [44]. This can be attributed to the main mechanism of chlorate formation at the two materials. At DSA anodes the process mainly occurred by the chemical reaction (r20), and appreciable amounts of ClO_3^- were detected only at low hydraulic residence times [44]. At BDD anodes, we should consider the further source of ClO_3^-, namely reactions (r14) and (r17), which occur in a thin layer adjacent to the anode surface, and mainly depend

on the concentration of radicals in the reaction layer and in turn, on the current density [38].

The good agreement between experimental and model predicted data obtained under all the working conditions considered, indicates that the effects of operative parameters, such as *Re*, current density and chloride concentration were correctly interpreted.

A similar approach was used to model the data obtained with solutions containing *M. aeruginosa*: the disinfection through bulk oxidants was assumed as main mechanism for inactivation of microalgae. The kinetics was modelled by a second order law ($R_{AL} = k_{AL} \cdot C_{OX} \cdot C_{AL}$) where the kinetic constant was an adjustable parameter. The best agreement between experimental and model predicted data was obtained with k_{AL}= 1 × 10^{-2} s^{-1}.

As the hydrodynamics is concerned, in the presence of algae, the system is a dilute suspension of cells in an electrolytic fluid: however, for diameter of the ducts more than two orders of magnitude greater than the size of a cell, the fluid can be regarded as homogeneous [57]. In the present case, the reactor can be considered as a porous medium with hydraulic diameter of 548 μm, two orders of magnitude greater than the diameter of *M. aeruginosa*; moreover, we should also consider the relative low content of cells and their density, similar to that of the electrolyte. Due to these reasons, the flow of the electrolyte with algae was modelled as that of a continuous fluid with properties of the BG 11 medium. *Figure 18* shows examples of values of chlorophyll-*a* removal obtained by steady state electrolyses under different operative conditions.

It is worth noting that the inactivation of *M. aeruginosa* was only appreciable at the lowest flow rate in the single pass configuration adopted.

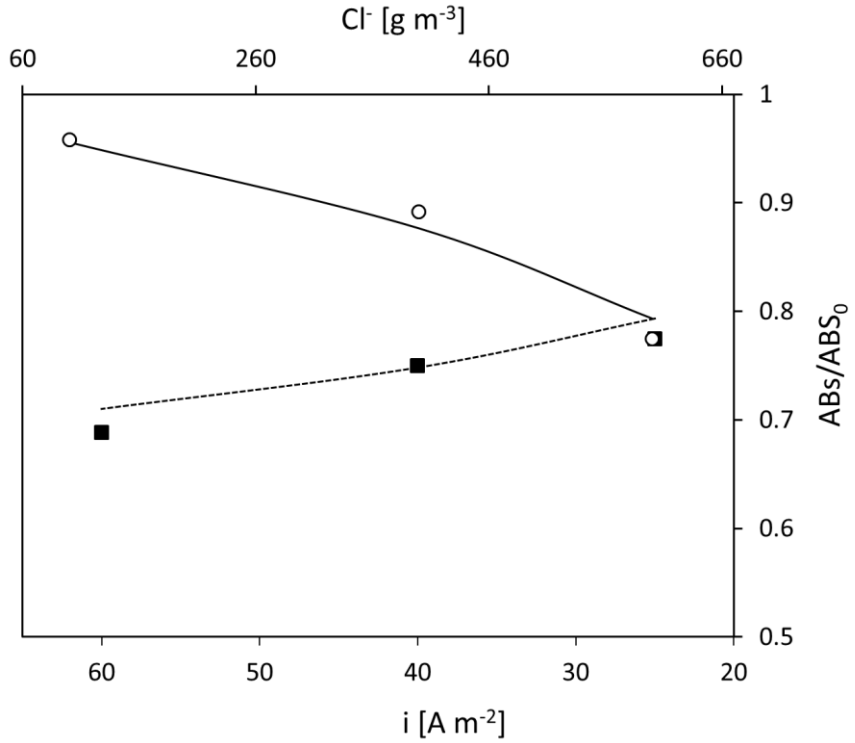

Figure 18. *Comparison between experimental (symbols) and model predicted (lines) steady state data of chlorophyll-a removal at Re = 10: i = 25 A m^{-2} and different chloride concentrations (empty symbols, upper x axis); 600 g m^{-3} of chloride and different current densities (full symbols, lower x axis) when BDD electrode was employed.*

Data obtained with i = 25 A m^{-2} and different Cl^- concentrations in the inlet (empty symbols, upper x axis) show the higher the concentration of chloride, the higher the effectiveness of the process towards inactivation of *M. aeruginosa*. The effect of current density (full symbols, lower x axis) is similar: the highest inactivation of microalgae was achieved under conditions of high current density (60 A m^{-2}), the concentration of chlorides in the inlet being the same.

As in the experiments in batch recirculated mode, the maximum inactivation was obtained under the experimental conditions most

favourable for high oxidants concentration in the reactor. The role of the active chlorine in algae inactivation processes was investigated in the literature [17], highlighting that nucleus, protoplasm and proteins of the cell membrane, can be damaged by active chlorine [58]. However, also under these conditions, the outlet concentrations of oxidants and chlorates were very low or below the detection limit: only electrolyses at i = 60 A m^{-2} of solutions containing 600 g m^{-3} of Cl^- allowed to detect about 1 mg dm^{-3} of oxidants.

The concentration of active chlorine is reduced by reaction with microalga, while the formation of chlorates is strongly decreased by the competition with algae inactivation, which reduces the active chlorine available, and by the possible reaction between the organic compounds and surface oxidants [42].

Based on these results, the main mechanism of inactivation is the reaction with bulk oxidants. This is furtherly confirmed by the good prediction of the model (lines), which in fact assumes the bulk oxidants as mechanism of *M. aeruginosa* inactivation.

The model has been calibrated with experimental values from a single couples of electrode stacks (anodic and cathodic), so that the inactivation of *M. aeruginosa* achieved is low. However, the inactivation requirements should be established depending on the specific problem: if the control of *M. aeruginosa* growth, to prevent the bloom, is the only requirement, then low inactivation rate can be sufficient.

Once validated, the model can be used to predict the behaviour of the system in a configuration in which several stacks in-series (alternating anodes and cathodes) are used. *Figure 19* shows the model predictions for different configurations and different concentrations of chlorides in the inlet at Re = 10 and i = 25 A m^{-2}. The values of energy consumption are also reported (the values for 1 stack can be referred to data in *Figure 18*), and were calculated with the experimental potential corresponded to 15 V.

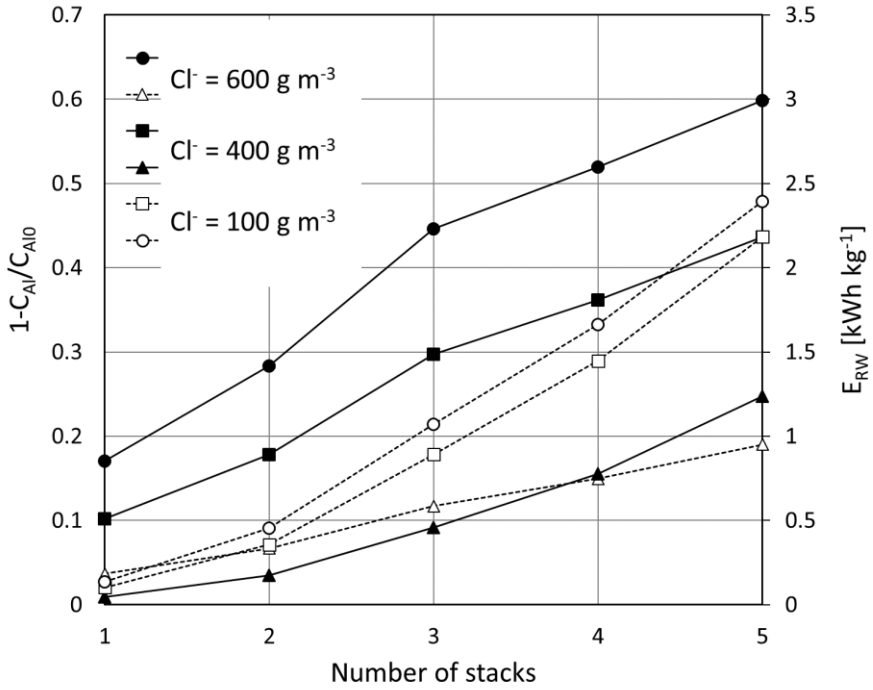

Figure 19. *Values of M. aeruginosa inactivation (full symbols, primary axis) and energy consumptions (empty symbols, secondary axis) predicted by the model for multi-stack reactor configurations at Re = 10 and i = 25 A m^{-2} and different inlet concentration of chlorides when BDD anode was used.*

The inactivation increases with the number of stacks, so that the reactor can be designed depending on the process requirements. The energy consumption is in the range 1.0–2.5 kWh per kg of *M. aeruginosa* removed: literature values for the specific process in continuous are not available for comparison, however we can consider that the concentration of *M. aeruginosa* considered corresponds to about to 1 kg m^{-3}, and the values are comparable to those obtained for batch recirculated processes [24,25].

Chapter 3

An integrated electrolysis-microbial fuel cell closed-loop system for *C. vulgaris* algae removal in water

3.1. Introduction II

3.1. Introduction II

Algae blooms pose a series of issues in wastewater treatment plants by interfering with both physical and chemical water purification processes, as it has been explained in 2.1. Therefore, costly dredging and disposal processes are consequently required [1] to successfully inactivate algae, such as the DE process that we have previously studied deeply throughout Chapter 2.

This process is mainly based on the use of electrochemically generated disinfectant agents, such us dissolved chlorine, chlorine dioxide, hypochlorous acid and hypochlorite ions for the removal of algae from aqueous media.

The main drawback of DE is, however, associated to its energy requirement, which would add to the great amount of energy that water treatments require. In the United States only, approximately 3–4% of the average daily electricity consumption is used for the treatment of wastewaters (WWs), which in turn results in the emissions of more than 45 million tons of greenhouse gases annually and a cost of approximately $4 billion (US EPA). Nonetheless, the DE of microalgae leads to the release of intracellular matter, such a lipids [59] or fatty acids [60] which could be exploited by using it as fuel in microbial fuel cells (MFCs) to produce useful electricity.

MFCs have attracted a lot of attention in the past decade as innovative renewable and carbon-neutral bio-electrochemical devices, capable of generating energy from WW effluents through the action of electroactive microorganisms [61–63]. In this particular type of fuel cell, microorganisms at the anode break the organic matter down into carbon dioxide, protons (H^+) and electrons (e^-). The electrons flow from the anode to the cathode generating an electrical current, while the protons flow across a proton exchange membrane to combine at the cathode with the electrons and an electron acceptor, usually oxygen, to form water.

MFCs have been proposed as an attractive means to treat WWs while generating electricity [61]. Contrary to anaerobic digesters, the energy conversion in MFCs is direct and, therefore, the theoretical energy

efficiency of MFCs is much higher. One of the biggest limitations of this technology that still prevents practical applications is, however, associated with the difficulty in the scaling-up [64]. The miniaturisation of the fuel cell design and the arrangement of multiple miniature units in stack is currently considered one of the most viable approach to overcome this limitation [65]. A wide variety of organic matter, originating from any sort of WW, has been tested as fuel in MFCs, and performance varied according to the biodegradability and bioavailability of the organic substrate [66]. Recently, algae have been considered as a new organic source for the anodic bacteria [67–69]. To improve the anaerobic biodegradability of microalgae biomass, pre-treatment techniques have been proposed to dissolve or disrupt the algae cell membrane and favour the accessibility of the bacteria to the organic matter [17,70–72].

In this work, we have integrated for the first time the DE step with the MFC technology with the aim of reducing the energy consumption of the electrolysis process and, therefore, the operating costs. In particular, an integrated closed-loop system is proposed, in which a fixed bed electrochemical reactor with three-dimensional electrodes for the microalgae electrolysis is coupled with a cascade of miniature air-cathode MFCs. *C. vulgaris* was used as the model microalgae since its resistance is lower than the blue-green algae, and may favour the release of intracellular matter, which would be used as fuel in the MFCs. The configuration of the DE system has been designed to minimise the presence of long-life oxidants in the outlet of the DE unit (the feed of the MFCs), to prevent any damage to the anodic biofilm inside the MFCs [44]. In particular, since active chlorine species are the most persistent among the oxidants electrogenerated in DE, boron-doped diamond was used as anode material, which combines high effectiveness in electrochemical treatments with relatively low catalytic activity towards active chlorine formation [29,38]. We also investigated the effect that increasing the electrode surface area as well as the number of single units in the cascade had on the overall algae removal efficiency and on the power generated by the MFC stack.

3.2. Materials and methods II

3.2. Materials and methods II

3.2.1. Algae culture

C. vulgaris green algae was kindly provided by the Department of Biology and Biochemistry, University of Bath (UK). WW from the Wessex Water treatment plant in Somerton (UK) was used as the growing media for *C. vulgaris*. The characteristics of the Somerton WW are reported in *Table 7*. The WW was ozonised and oxygenated prior to use. *C. vulgaris* was cultivated in 1 l flasks under continuous fluorescent light at 25 ± 1°C and at 43% of humidity. All experiments were carried out when *C. vulgaris* was in the *log-growth* stage, which corresponded to an algal concentration of 15 x 10^9 cells dm^{-3} and to a COD value of about 35 ± 7 mg dm^{-3}.

Table 7. *Characteristics of the Somerton wastewater.*

Parameter	Value
pH	7 ± 0.5
Conductivity (µS)	810 ± 50
COD (mg dm^{-3})	35 ± 7
Phosphate (mg dm^{-3})	3.2 ± 0.9
Nitrate (mg dm^{-3})	21.3 ± 3
Total Nitrogen (mg dm^{-3})	27 ± 5
Total Suspended Solids (mg dm^{-3})	1

3.2.2. Apparatus

3.2.2.1. Electrochemical cell and procedures

DE experiments were performed with the fixed bed electrochemical reactor equipped with 6 discs in-series of conductive diamond anode (BDD) previously described in 2.2.2, with the system configured as in *Figure 2A*. The experimental conditions for the batch recirculated electrolysis runs are reported in 2.2.3. It is worth noting that no chlorides ions were added in the electrolyte for this study.

C. vulgaris removal and oxidants concentration were monitored by measuring the absorbance of the chlorophyll-*a* pigment and the DPD colorimetric technique, respectively, as described in 2.2.4.

3.2.2.2. Microbial fuel cell

Two designs of miniature air-cathode MFCs were used in this study, fabricated as previously reported [65]. The anodic channel was made of polydimethylsiloxane silicon (PDMS, Ells Worth Adhesives) with a 10:1 ratio. Carbon cloth (untreated carbon cloth type B, E-Tek, USA) was used as both the anode and the cathode electrodes. Nafion® (115, Sigma-aldrich) was used as the proton exchange membrane, and was hot pressed to the cathode by applying a pressure of 3 bar for 90 s at 130°C. *Figure 20* shows schematic and pictures of the two devices used. Two cell lengths were considered: 4 and 8 mm. As a result, the electrode nominal surface area was respectively of 0.16 and 0.32 cm^2, corresponding to anodic volumes of 0.048 and 0.096 cm^3, respectively. The inter-electrode gap was of 0.3 cm. Titanium wire (Advent Research Materials, diameter 0.2 mm) was used as electrical contacts.

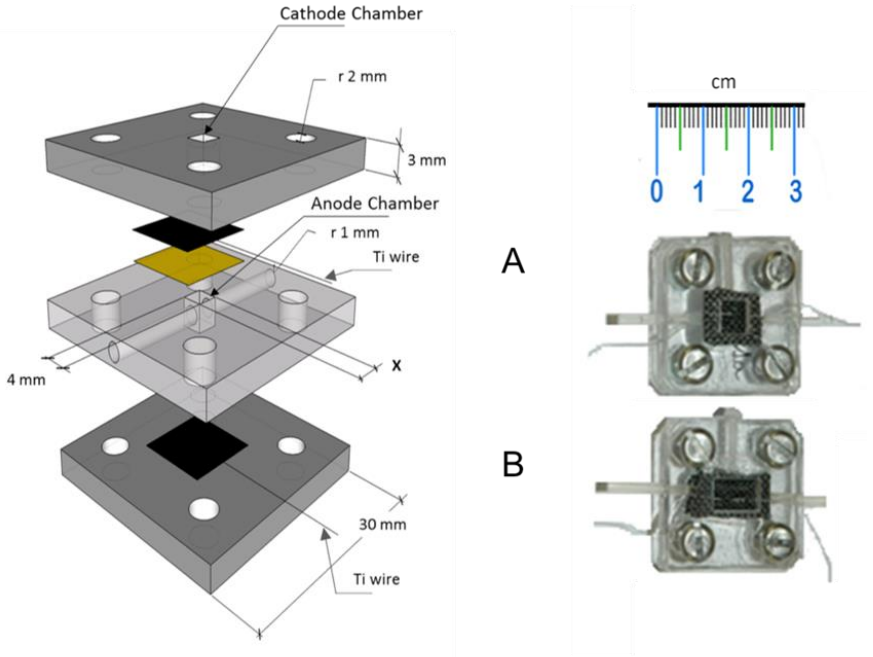

Figure 20. *Schematic and photograph of the fuel cell devices used in this study. Carbon cloth electrode surface area: 0.16 cm^2 (A) and 0.32 cm^2 (B).*

3.2.3. Fuel cell operation

The anode and the cathode electrodes of each air-cathode MFC were connected through a fixed external resistor (R_{ext}) and to a data acquisition system (PicoLog 1012) and the cell voltage of each MFC was recorded at intervals of 10 s.

The maturing of the electrochemically anaerobic active bacteria at the anode was performed by feeding the fuel cell (batch recirculating mode at a flow rate of 0.4 cm^3 min^{-1}) with artificial wastewater (AWW), containing 2% (v/v) of anaerobic sludge (Wessex Water, Scientific Laboratory in Saltford, UK). AWW was prepared by adding to distilled water (all values in mg dm^{-3}): $(NH_4)_2SO_4$ 200; $MgSO_4{\cdot}5H_2O$ 59; $MnSO_4{\cdot}H_2O$ 6; $NaHCO_3$ 130; $FeCl_3$ 3; $MgCl_2{\cdot}6H_2O$ 7. Potassium acetate at a concentration of 9.81

g dm^{-3} was used as the carbon source. The resulting COD value was 2.200 ± 200 mg dm^{-3}, and the pH of the solution was adjusted to 7 ± 0.5 with HNO_3 (0.1 M). The solution, replaced on a daily basis, was sterilised and purged with N_2 prior to its use. After approximately one week of operation, the output voltage reached a stable value and the enrichment phase was considered concluded. The MFCs were therefore hydraulically assembled in-series, while still electrically independent from each other, and fed with electrolysed algae under a continuously recirculated flow rate of 0.4 cm^3 min^{-1} (see *Figure 21*). Under this flow, the hydraulic retention time of each MFC was of 7.2 or 14.4 s, according to the length of the anodic chamber.

Polarisation experiments were performed by connecting the MFCs to a series of external loads, varying from 10 Ω to 1000 kΩ, controlled by an external variable resistor (RS-200 Resistance substitute, IET Labs Inc., USA), and by measuring the pseudo steady state output potential after 10 min. Before the test, the MFC was left under open circuit for no more than 2 hours to allow a steady state open circuit voltage (OCV) to develop. Ohm's law ($I = {\Delta E_{CELL}}/{R_{ext}}$) was used to determine the corresponding current (I) at each external load value.

The volumetric power density, P, (W m^{-3}) generated by each MFC was calculated as:

$$P = \frac{\Delta E_{CELL} \cdot I}{V} = \frac{\left(\frac{\Delta E_{CELL}{}^2}{R_{ext}}\right)}{V} \quad (13)$$

The energy, E, (W h m^{-3}) produced by each MFC, over the time t, was calculated as:

$$E = \int_0^t \frac{\Delta E_{CELL} \cdot I}{V} dt \quad (14)$$

The overall energy generated by the MFC stack was calculated as the sum of energy produced by each single MFC.

3.2.4. Set-up and operation of the closed-loop integrated system

Figure 21 shows the set-up of the integrated batch recirculated system. The electrolysis unit (2) was inserted into a batch recirculating hydraulic circuit and pumped with a *C. vulgaris* algae solution (35 mg COD dm^{-3}, volume (*V*): 200 cm^3) (1) at *Re* = 13. An electric field, parallel to the fluid flow, was applied by setting a current density of 25 A m^{-2} with a power supply (3), leading to a cell voltage of 12 V. The electrolyte (1) was also fed into the cascade of MFCs (4) at a flow rate of 0.4 cm^3 min^{-1} with a multichannel peristaltic pump equipped with 2-stop tubing. The electrolysis unit was operated for an hour. Afterwards, the solution in reservoir (1) was recirculated to the cascade of MFCs for up to three days.

To test the effect of numbering up the fuel cell in the cascade on the algal inactivation and energy generation, the stack (4) was made up of either three or five MFCs. The MFCs in the stack were electrically independent from each other to monitor individually their performance.

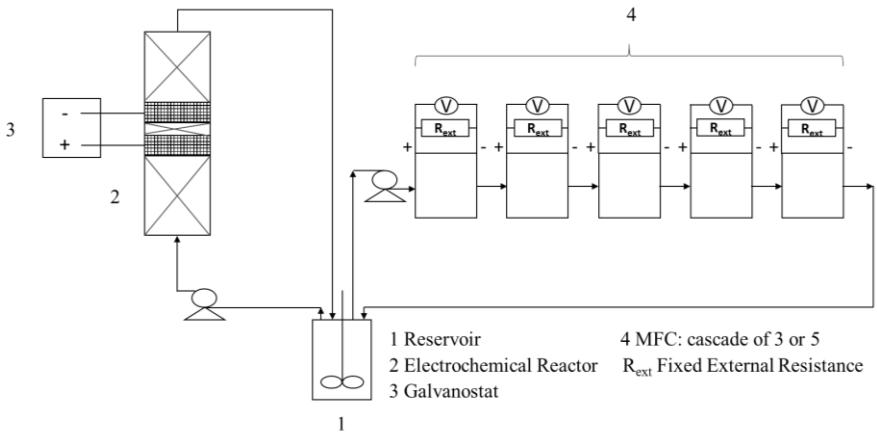

Figure 21. *Set-up of the combined system. The algae solution (1) is recirculated into the electrolysis unit (2) as well as into the cascade of MFCs (4). The cascade consisted of either three or five microbial fuel cells hydraulically connected in-series while, electrically independent.*

3.3. Results and discussion II

3.3. Results and discussion II

Data obtained for the *C. vulgaris* inactivation during chloride-free electrolyte-batch recirculated electrolyses can be found in 2.3.1.1. These preliminary runs allowed establishing the operative conditions that were adopted for the experiments carried out during the integrated system. The applied current density and the flow rate chosen for the combined DE-MFC system were i = 25 A m^{-2} and Re = 13, which lead to a relatively low energy requirement (6 kWh m^{-3}), corresponded to a 50% of the normalised removal of chlorophyll-*a* over an hour of operation, by the electrolysis unit.

The outlet from the electrolysis unit was recirculated into a stack of MFCs hydraulically connected in-series for a total of 3 days. The effect of two variables on the stack performance was investigated: the MFC characteristic length along the direction of the flow, which affects the surface area of both the anode and the cathode; and the number of MFC devices in the stack. In particular, two lengths were tested, 4 and 8 mm, leading to a surface area of both electrodes of 0.16 and 0.32 cm^2 respectively, and two different MFC stacks were investigated, one made up of three devices and the other of five.

The MFCs were enriched individually, with anaerobic sludge and AWW containing acetate as carbon source, and hydraulically connected in-series after approximately one week when a steady state current was observed. Polarisation tests performed after one week of operation reveal a peak power output of 0.064 ± 0.003 µW cm^{-2}, for an external load of 250 kΩ, for the case of a surface area of 0.16 cm^2. For the fuel cells with an electrode surface area of 0.32 cm^2, the maximum power was an order of magnitude higher: 0.293 ± 0.005 µW cm^{-2}, for an external load of 45 kΩ. The different value of optimal R_{ext} observed for the specific MFC design, was applied to the respective fuel cell prior to assembling them in a stack. Once integrated in the closed-loop circuit, the MFCs were fed with the algal solution from reservoir 1 (*Figure 21*). Although the DE unit was activated over the first hour of operation only, the cells were also running during the subsequent three days. After that, the MFCs were disassembled and a new batch recirculated of experiments was performed.

The performance of the MFCs stack in terms of electricity generation over three days was also investigated. *Figure 22* and *Figure 23* show the change in the power density with the time for both the three-MFC stack and five-MFC stack, respectively, with the electrodes surface area of 0.32 cm^2.

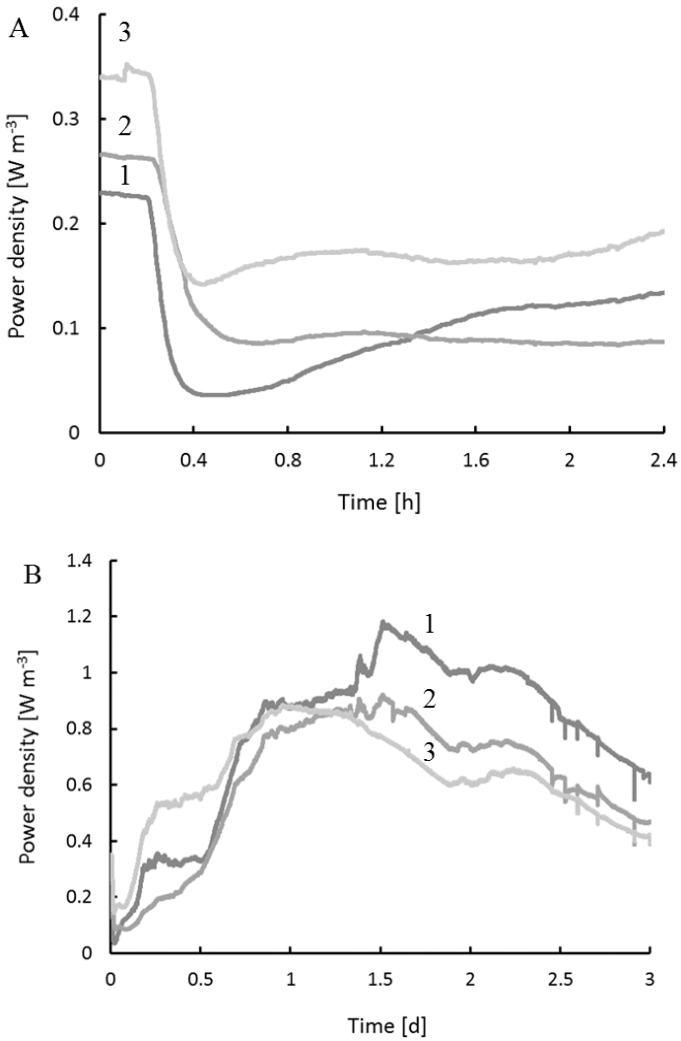

Figure 22. *Power density output with time for each individual microbial fuel cell in the stack, over approximately the first 2.5 hours (A) and three days (B) of operation. Numbers indicate the position of the MFC in the stack with 1 being the first MFC along the direction of the flow. The surface area of the electrodes was equal to 0.32 cm^2.*

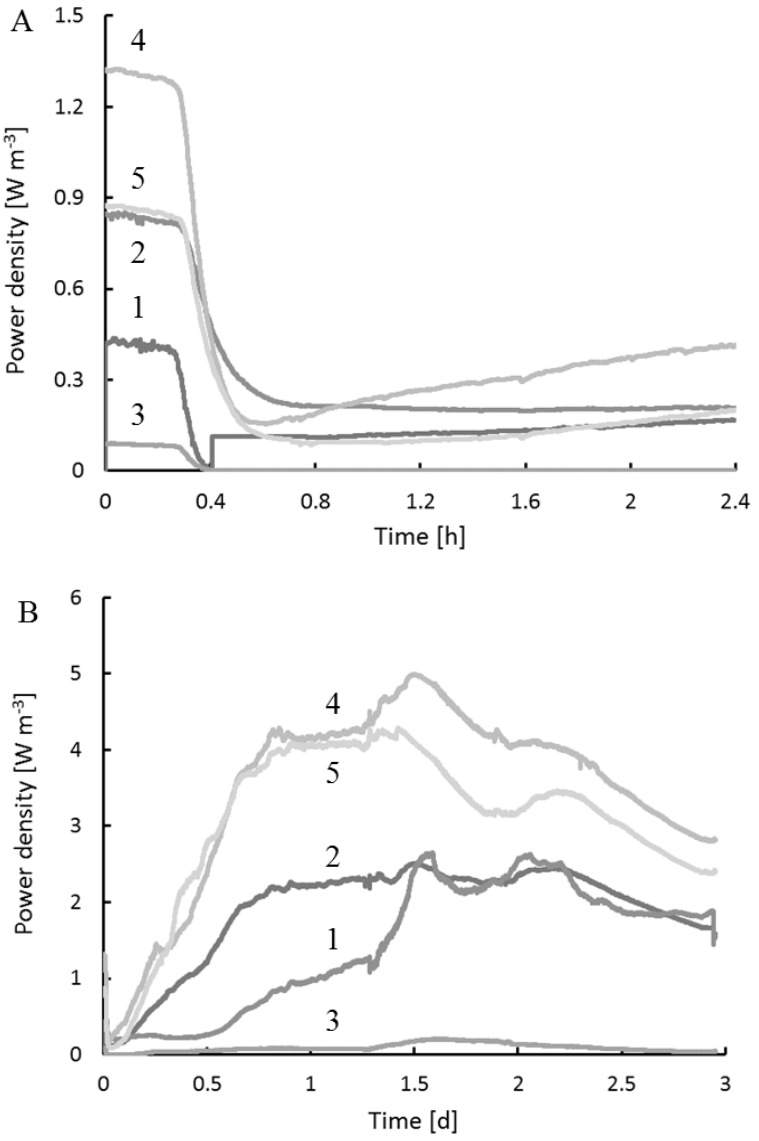

Figure 23. *Power density output with time for each individual microbial fuel cell in the stack, over approximately the first 2.5 hours (A) and three days (B) of operation. Numbers indicate the position of the MFC in the stack with 1 being the first MFC along the direction of the flow. The surface area of the electrodes was equal to 0.32 cm^2.*

After the first 15 minutes of operation, a decrease in the power output was observed. This power drop was attributed to the drastic change in the COD value of the feeding solution, which decreased from value of 2200 mg dm^{-3} (AWW containing acetate and anaerobic sludge) to only 35 mg dm^{-3} (AWW with an initial concentration of *C. vulgaris* equal to 15 x 10^9 cells dm^{-3} in the DE unit inlet). On the other hand, the conductivity (810 ± 50 µS) and the pH (7 ± 0.5) were the same for both the AWW and the algae solution. Therefore, the power drop was associated only to the change in the concentration of organic carbon in the new feeding solution and to the switch of fuel from acetate to the organics released from the broken cells, which might be complex molecules, more difficult to digest. Moreover, during this initial period, it is likely that the feed into the MFCs would be still characterised by a large amount of unbroken cells. On the one hand, this would mean a low concentration of organic carbon in the feed, on the other hand the living algal cells might inhibit the metabolism of the anodic bacteria, thus further decreasing the output power [73]. Power outputs close to zero have been previously observed when bacteria-enriched MFCs were suddenly fed with fresh algae cells, thus confirming this hypothesis [69].

Once the electrolysis unit was discarded (i.e. after 1 hour of operation), the power output started to increase, reaching a peak after approximately one day of operation, and then it slowly decreased.

For the case of the three-MFC stack (*Figure 22A*, and *Figure 22B*), no marked difference in the performance of each fuel cell was observed. The peak power density was of 1 W m^{-3} with a 0.17% of variation. In the case of the five-MFC stack, the performance of the last fuel cells along the cascade, MFC4 and MFC5 (*Figure 23A*, and *Figure 23B*) was different. The peak power in this case was of 5 and 4.11 W m^{-3} for MFC5 and MFC4, while for MFC1 and MFC2 it was respectively of 2.5 and 2.7 W m^{-3}. Note that the poor performance of MFC3 was caused by heavy leaking during the experiment.

Winfield et al. reported the effect that different organic loads have on the behaviour of the individual MFCs in a continuous-flow cascade system [74]. Usually, for easy-to-digest organics, the MFCs down the chain perform worse than the MFCs positioned at the beginning of the cascade, due to fuel depletion. On the other hand, the better performance of MFC4

and MFC5 in this case might be attributed to the fact that the first cells in the cascade help with the breaking down and release of organic molecules from the algae cells, thus leading to an increased amount of available and easy-to-digest organic source to the last MFCs along the cascade [71]. According to the results obtained, it seems that when only three MFCs are used, this phenomenon is not as marked as the case of five cells.

Figure 24 reports the average change in the COD value of the recirculating solution with the time.

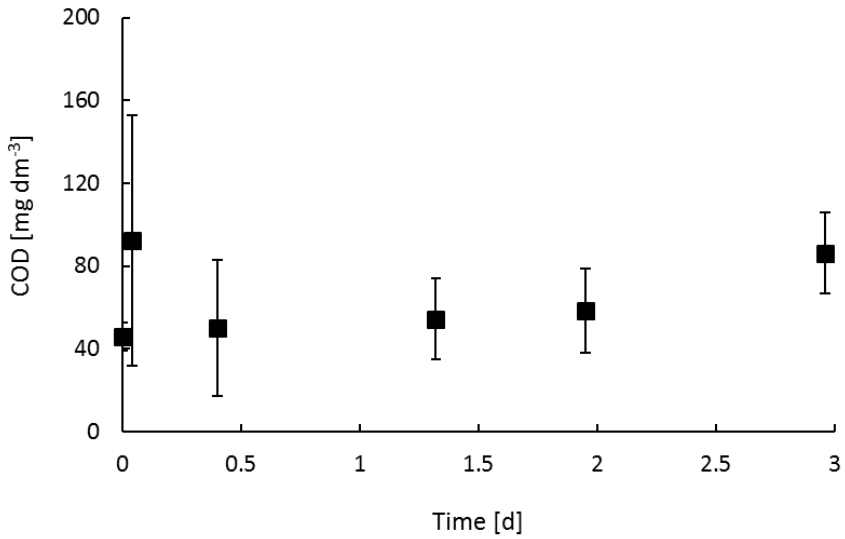

Figure 24. *Average values of the COD for the recirculated electrolysed C. vulgaris algae solution in the stacks of three and five MFCs for both the electrode areas tested.*

As shown, a peak of COD (92.5 ± 60.5 mg dm^{-3}) was observed after the first hour of operation caused by the electrolysis of the algal cells by the DE unit. The COD then stabilised to 55 mg dm^{-3} for approximately 1.5 days and then slowly increased. This increase with time is probably caused by the release of organics and metabolites due to the bacterial action in the MFC. Although this trend in the COD concentration was highly

reproducible for each MFC stack studied, the stack with the MFCs with the electrode surface area of 0.32 cm^2 led to COD values approximately 1.3 times higher (69 and 91 mg dm^{-3} for the three- and five-MFC stack respectively).

Figure 25 compares the cumulative electricity generated over a period of 3 days by each MFC in the four different stacks studied, obtained by varying the number of MFCs and the electrode surface area. It can be noted that, in the case of MFCs with an electrode surface area of 0.16 cm^2, if we exclude MFC5 (poorly performing because of leaking/damage), no marked difference in the performance of each MFC were observed for both in the case of three- and five-MFC cascade. This might be due to the fact that the larger electrode surface area was associated with an increase in the retention time (14.4 seconds versus 7.2) and, consequently, with a better digestion of the algal cells and in turn an increase the amount of ready-to-be oxidised organics for the anodic biofilm of the MFCs down the chain.

The active surface area of the electrodes has an influence on the performance of the MFCs [61,65,75,76]. For the three-MFC stack, when the electrode surface area was of 0.16 cm^2 the average power output was 82% lower than when the surface area was double. In the miniature MFC devices used in this study, the increase in the electrode surface area while keeping constant the cross sectional area produced a decrease of the diffusion resistance [65]. According to the results obtained, this improvement in the mass transport has a benefit on both the algae treatment and the energy production.

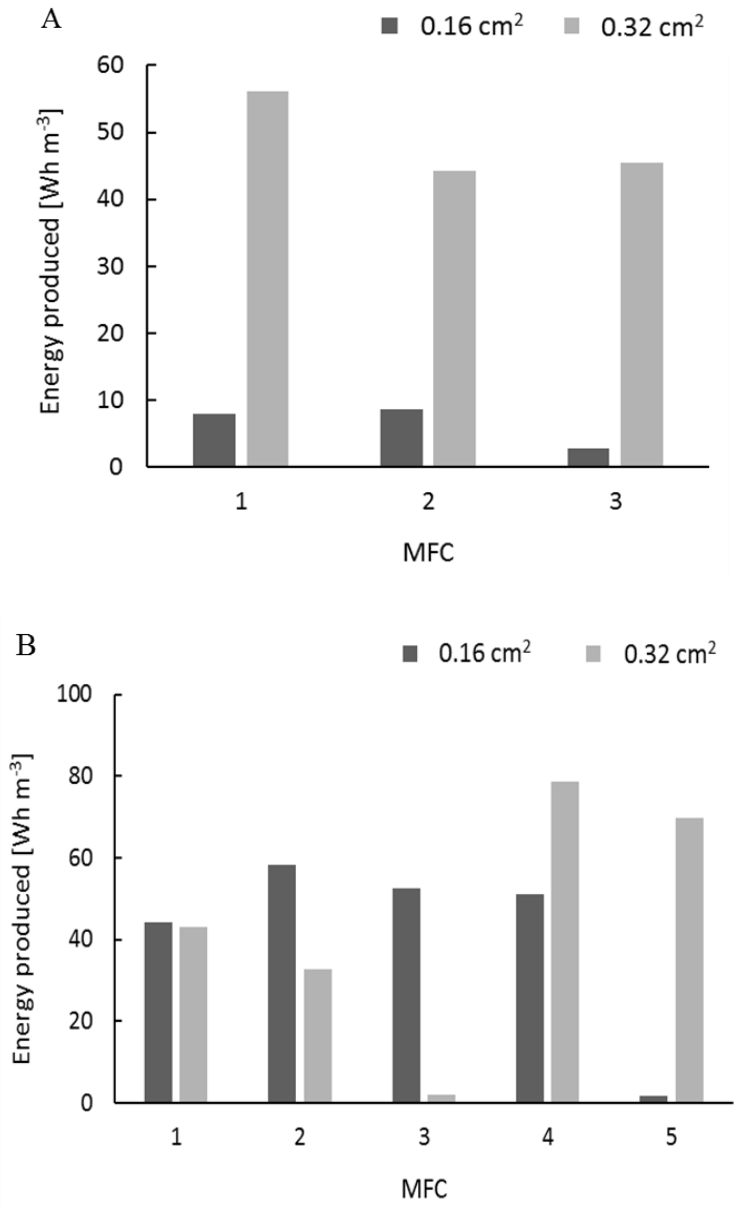

Figure 25. *Amount of cumulative energy generated by each microbial fuel cell in the cascade-stacks of: A) three, and B) five microbial fuel cells using two different anodic surface areas over three days.*

Figure 26 shows the total energy generated by the MFC stacks, calculated as the mathematical sum of the cumulative energy produced by each MFC unit in the specific stack configuration.

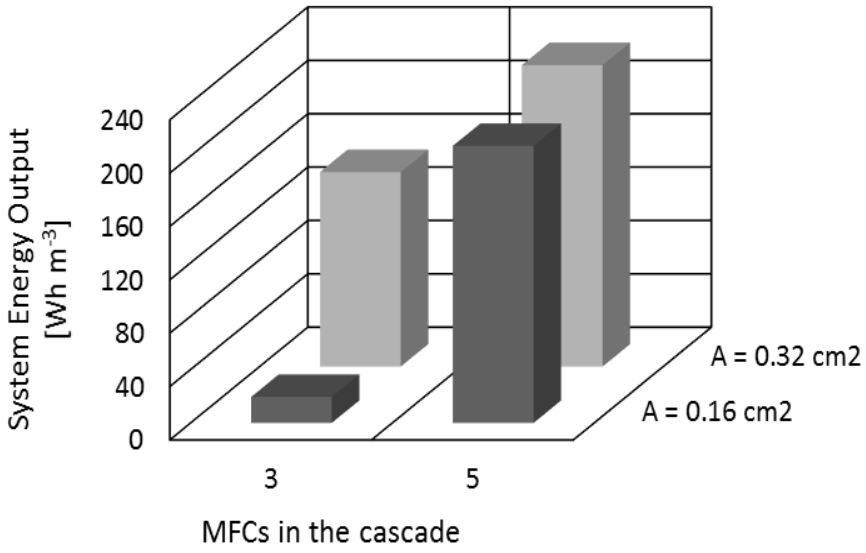

Figure 26. *Total cumulative energy generated by the several MFC stacks investigated.*

As shown, the increase on the number of MFCs in the stack leads to higher power output levels for the case of the two anodic surface areas investigated. The use of sequentially positioned MFCs may maximise the oxidation of the organic matter [77] and in turn, an increase of the power production can be expected. The most significant increase (11 times the initial value) in the energy output was observed when the smallest electrode area (0.16 cm^2) was employed. A much lower, but still a positive effect of increasing the number of MFCs in the stack was also observed when the electrode surface area was 0.32 cm.

Chapter 4

Conclusions

According to the objectives introduced at the beginning of this thesis, several conclusions can be drawn, in which a packed bed electrochemical reactor, with 3D electrodes of Nb grids coated with conductive diamond (BDD) and expanded meshes of commercial Ir/Ru mixed oxides (dimensionally stable anodes, DSA) as anodes, was used to investigate the treatment of water containing *M. aeruginosa* and *C. vulgaris* algae.

The removal efficiency of *C. vulgaris* in a chloride-free solution for water disinfection process may be attributed to the synergistic effect owing to the applied electric field and the very high concentration of oxidants in the anode zone. Moreover, in the presence and absence of algae the difference in oxidant concentration was only insignificant, further confirming that the reaction with bulk oxidants might not contributed to the removal process.

On the other hand, the removal efficiency of *M. aeruginosa* in water disinfection process may be related to the synergistic effect of electrogenerated oxidants produced from the chloride ions and electric field, but the experimental results demonstrated that the main inactivation mechanism is the bulk disinfection by the mixture of oxidants generated during the process, mainly constituted by active chlorine species electrogenerated at the anode surface. Chlorates were the only oxidation products of active chlorine in detectable amount: the measured concentrations of chlorates in the inlet stream at BDD anodes were slightly higher than those obtained at DSA ones [44].

The presence of *M. aeruginosa* algae in aqueous media resulted in a very low concentration of oxidants and disinfection by-products, such as chlorates, usually found during electrolysis with BDD anodes. Only at the most favourable experimental conditions for the chlorates formation of high electric field and high Cl^- concentration in the inlet of the reactor allowed to detect at least 1 mg dm^{-3} of oxidants.

Similar results were achieved with electrolyses in continuous mode. The steady state results obtained when BDD anode was employed can be compared with those ones when the electrolysis unit was equipped with DSA anodes. Although the mechanism of formation of oxidising compounds is significantly different at mixed oxide and diamond

electrodes, both materials could be effective to remove *M. aeruginosa*, providing sufficient amount of oxidants.

Based on steady-state experimental results, a dispersed plug flow model was used to numerically predict the behaviour of the system. The model predictions were compared with the experimental data: the model effectively represented the process, allowing the prediction of the outlet concentration of *M. aeruginosa*, residual disinfectant and disinfection by-products under different operative conditions. From the model predictions we can obtain a current related to the generation of bulk oxidants from 1 to 7% of the total, and dependent on the Cl^- concentration. The corresponding currents for chlorates generation were one order of magnitude less. The model was also used to simulate a multi-stack reactor, which allows obtaining higher and controllable extent of *M. aeruginosa* inactivation.

In addition, this study intended to provide preliminary results for a cost-effective and green solution to the treatment of *C. vulgaris* algae contaminated water systems. An innovative approach, based on the integration of the electrolysis unit equipped with conductive diamond anodes, with a stack of miniature single chambered air-cathode microbial fuel cells (MFCs), was proposed. This integrated system allowed the simultaneous treatment of algal biomass in wastewaters and energy generation. With our work, we not only demonstrated the effectiveness of such approach, but, with the aim of guiding on the design of such systems, we also investigated on the effect that key features of the MFCs stack have on performance.

The lower energy demand of the integrated system leads to an energy cost of 0.9 € m^{-3}, which considering an energy price of 0.134 €kW h (Eurostat 2014), is 50% less than the operating cost of the single direct electrolysis (DE) unit. Moreover, the generated cumulative power output of up to 226 Wh m^{-3}, when the MFCs were fed with the electrolysed algae over a period of three days, allowed to furtherly reduce the electrical energy consumed by DE reactor of about 20%.

These results are encouraging: by further improving the design of the MFC stack, a self-sustainable process could be obtained. Current water treatment systems are unsustainable, as they require consistent amounts of energy.

This great energy demand not only has a high impact on the economy of our cities, but, considering that it is currently addressed by fossil fuels, it also has important environmental consequences. As such, our work will help to transform wastewater from an energy issue to an energy source.

Appendix

Supporting materials

I. Algae growth curve and concentration

Figure 27A shows a typical microalgae growth curve: in particular, this curve was obtained for the *M. aeruginosa* algae under the conditions reported in 2.2.1. As can be seen, there are 4 reasonably well defined phases of algal growth: lag (1), exponential (2), stationary (3), and death (4).

- Lag phase: the inoculum is being acclimatised to the growing culture BG 11.
- Exponential phase: is known as the *log-growth* phase, in which the increase of the biomass over time happens. Cell count or dry weight are common units of biomass determination.
- Stationary phase: net growth is zero, and within a few hours cells may undergo dramatic biochemical changes.
- Death phase: when vegetative cell metabolism can no longer be maintained the death phase of a culture is generally very rapid. Cultures of this species will lose their pigmentation and appear washed out.

Figure 27B represents the algae concentration, measured by cell counting (equation (15)) employing an optical microscope, during the *log-growth* phase of algae.

$$\frac{Cells}{mm^3} = \frac{Counted\ cells}{Counted\ surface\ (mm^2) \cdot Chamber\ depth\ (mm) \cdot Dilution} \qquad (15)$$

where, counted surface and chamber depth are 4 mm^2 and 0.1 mm, respectively.

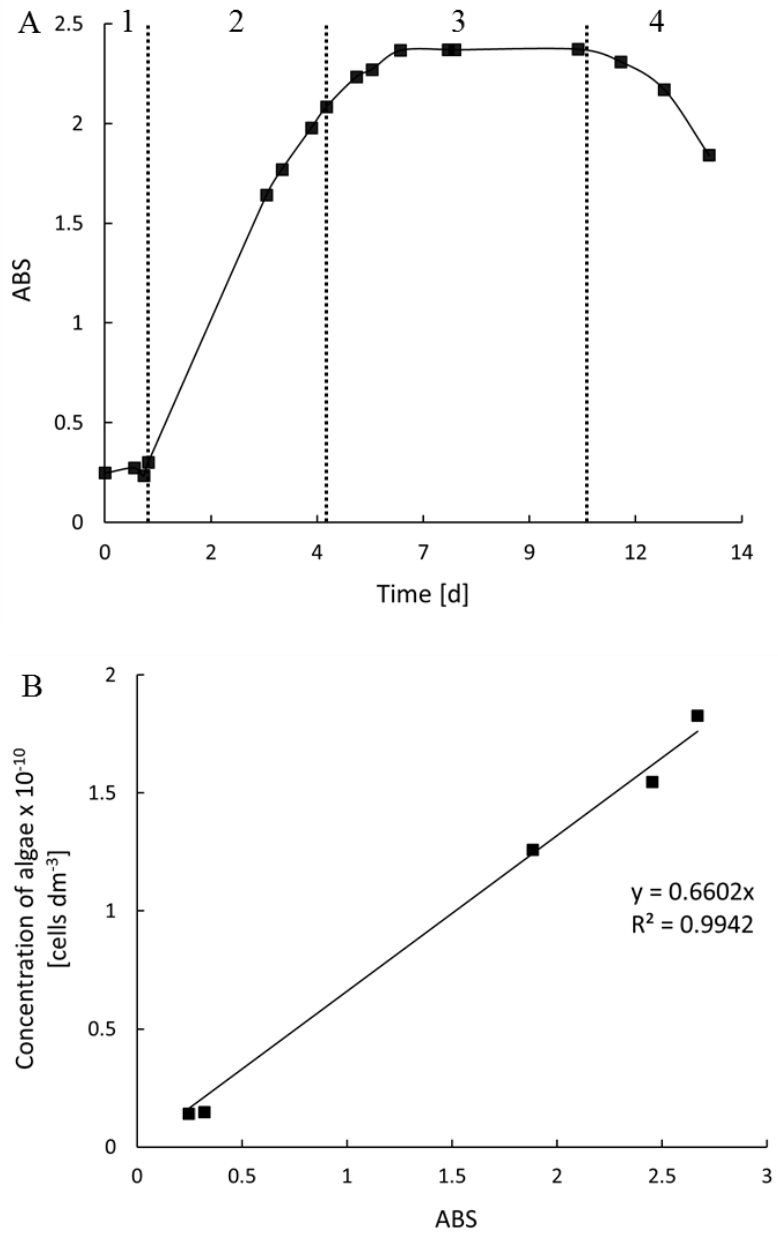

Figure 27. *M. aeruginosa microalgae growth curve (A) and the algae concentration in the log-growth phase (B). Phases for (A): Lag (1), exponential (2), stationary (3), and death (4) phase.*

II. Mass transfer characterisation

Cathodic mass transfer coefficients (k_m^c) were obtained by using the linear sweep voltammetry (LSV) technique.

First, cyclic voltammetry (CV) of the redox ferricyanide/ferrocyanide couple, by means of a potentiostat (Autolab, Metrohm), under the operative conditions written in 2.2.5 was performed in order to know what the reduction peak of $K_3Fe[CN]_6$ was (*Figure 28*).

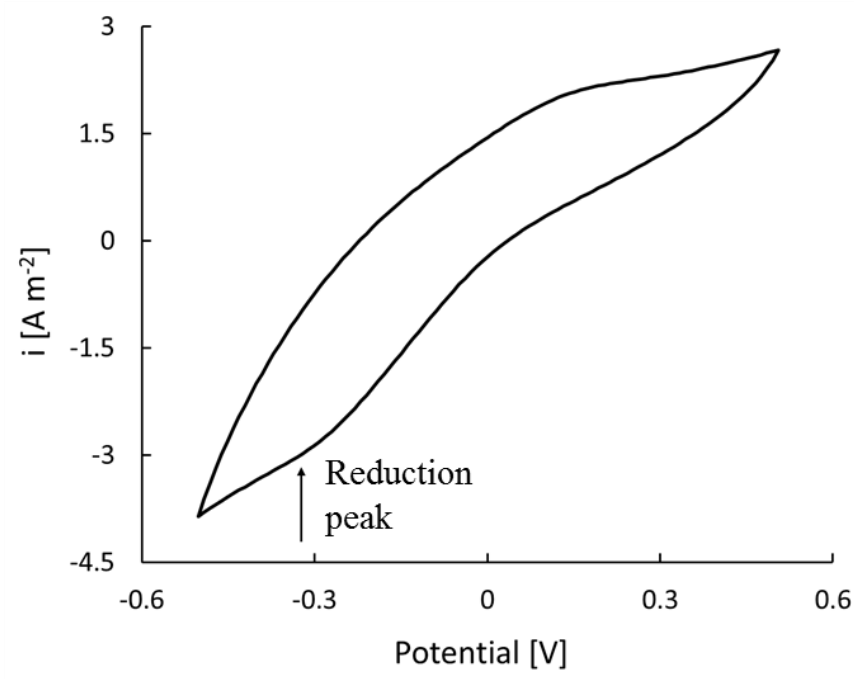

Figure 28. *Cyclic voltammogram of the standard redox ferricyanide/ferrocyanide couple at scan rate of 0.5 mV s^{-1}.*

Then, a LSV was carried out at different *Re* values (10–120) under constant scan rate (0.5 mV s^{-1}) so that the limiting current density (i_L) could be measured (*Figure 29*).

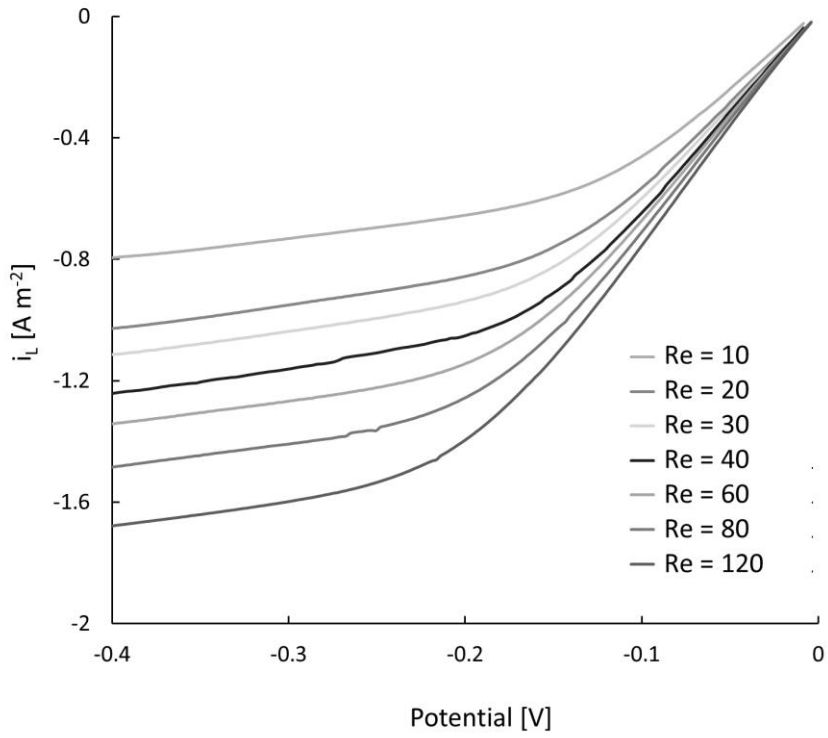

Figure 29. *LSV at 0.5 mV s^{-1} of scan rate under different flow rates for the standard redox ferricyanide/ferrocyanide couple.*

Once the i_L is known, the values of $k_m{}^c$ can be calculated from equation (5) at the relevant *Re* numbers, employing the physical properties of ferrocyanide solution, which behaves as diluted aqueous solutions: μ/ρ = 0.952 x 10^{-6} m^2 s^{-1}; D = 6.41 x 10^{-10} m^2 s^{-1}.

Sherwood and Schmidt dimensionless numbers were then calculated with the following equations:

$$Sh = \frac{k_m^c \cdot d}{D} \quad (16)$$

$$Sc = \frac{\mu}{\rho \cdot D} \quad (17)$$

III. Model equations

The system was modelled by combining the main kinetic equations with an axial-dispersed plug flow model, which accounts for the non-ideal flow conditions. The reactor was modelled as two reaction zones, the first representing the anode packing and the second the cathode packing, and with three flow zones, upstream, downstream and between the reaction zones. The kinetic equations can be written according to the assumptions of the model (reactions in brackets refer to *Table 1*):

- Anodic generation of bulk oxidants (r6–r9)

$$R_1 = \frac{i}{n_e \cdot F} \cdot a_A \cdot \varepsilon_{OX} \quad (18)$$

- Chemical decay of bulk oxidants (r19, r20)

$$R_2 = k_D \cdot C_{OX} \quad (19)$$

- Anodic generation of chlorates (r14, r17)

$$R_3 = \frac{i}{n_e \cdot F} \cdot a_A \cdot \varepsilon_{ClO_3^-} \quad (20)$$

- Cathodic reduction of bulk oxidants

$$R_4 = -a_C \cdot k_m \cdot C_{OX} \quad (21)$$

Under one-dimensional approximation, the differential equation bellow represents the mass balance of the ith species involved in the process:

$$\nabla(-\nabla D C_i) = R_i - v\nabla C_i \quad (22)$$

The term R_i can be written as

- Anode packing

$$R_{OX} = R_1 - R_2 \quad (23)$$

$$R_{ClO_3^-} = R_3 + {}^1\!/_3\, R_2$$

- Cathode packing

$$R_{OX} = R_4 - R_2 \quad (24)$$

$$R_{ClO_3^-} = {}^1\!/_3\, R_2$$

- Flow zones

$$R_{OX} = -R_2 \quad (25)$$

$$R_{ClO_3^-} = {}^1\!/_3\, R_2$$

Therefore, the resulting global mass balance is as follows:

$$R_{OX} = \frac{i}{n_e \cdot F} \cdot a_A \cdot \varepsilon_{OX} - a_C \cdot k_m \cdot C_{OX} - 3k_D \cdot C_{OX} \quad (26)$$

$$R_{ClO_3^-} = \frac{i}{n_e \cdot F} \cdot a_A \cdot \varepsilon_{ClO_3^-} + k_D \cdot C_{OX} \quad (27)$$

The boundary conditions were the following:

$$C_i = 0 z = 0 \quad (28)$$

$$\nabla(-\nabla D C_i) = 0 z = L$$

The numerical model was built and solved with the commercial software COMSOL Multiphysics®, combining the kinetics with flow in porous media.

Bibliography

[1] E. Dittmann, C. Wiegand, Cyanobacterial toxins - Occurrence, biosynthesis and impact on human affairs, Mol. Nutr. Food Res. 50 (2006) 7–17. doi:10.1002/mnfr.200500162.

[2] J. Ma, W. Liu, Effectiveness and mechanism of potassium ferrate (VI) preoxidation for algae removal by coagulation, Water Res. 36 (2002) 871–878. doi:10.1016/S0043-1354(01)00282-2.

[3] V.H. Smith, G.D. Tilman, J.C. Nekola, Eutrophication: Impacts of excess nutrient inputs on freshwater, marine, and terrestrial ecosystems, Environ. Pollut. 100 (1998) 179–196. doi:10.1016/S0269-7491(99)00091-3.

[4] G. Zanchett, E.C. Oliveira-Filho, Cyanobacteria and cyanotoxins: From impacts on aquatic ecosystems and human health to anticarcinogenic effects, Toxins (Basel). 5 (2013) 1896–1917. doi:10.3390/toxins5101896.

[5] M.R.T. Dale, Book Reviews, J. Ecol. 45 (2000) 366–370.

[6] L. Chen, J. Chen, X. Zhang, P. Xie, A review of reproductive toxicity of microcystins, J. Hazard. Mater. 301 (2016) 381–399. doi:10.1016/j.jhazmat.2015.08.041.

[7] Y. Liu, J. Zhang, B. Gao, S. Feng, Combined effects of two antibiotic contaminants on *Microcystis aeruginosa*, J. Hazard. Mater. 279 (2014) 148–155. doi:10.1016/j.jhazmat.2014.07.002.

[8] P.T. Orr, G.J. Jones, Relationship between microcystin production and cell division rates in nitrogen-limited *Microcystis aeruginosa* cultures, Limnol. Oceanogr. 43 (1998) 1604–1614. doi:10.4319/lo.1998.43.7.1604.

[9] S. Corbel, C. Mougin, N. Bouaïcha, Cyanobacterial toxins: Modes

of actions, fate in aquatic and soil ecosystems, phytotoxicity and bioaccumulation in agricultural crops, Chemosphere. 96 (2014) 1–15. doi:10.1016/j.chemosphere.2013.07.056.

[10] K.J. Ives, The significance of surface electric charge on algae in water purification, J. Biochem. Microbiol. Technol. Eng. 1 (1959) 37–47. doi:10.1002/jbmte.390010105.

[11] P.M. Bradley, Plant hormones do have a role in controlling growth and development og algae, J Phycol. 27 (1991) 317–321. doi:10.1111/j.0022-3646.1991.00317.x.

[12] A.K.-Y. Lam, E.E. Prepas, D. Spink, S.E. Hrudey, Chemical control of hepatotoxic phytoplankton blooms: Implications for human health, Water Res. 29 (1995) 1845–1854. doi:10.1016/0043-1354(94)00348-B.

[13] G. Joh, J. Lee, Cyanobacterial biofilms on sedimentation basins in a water treatment plant in South Korea, J. Appl. Phycol. 24 (2012) 285–293. doi:10.1007/s10811-011-9678-z.

[14] B. Ghernaout, D. Ghernaout, A. Saiba, Algae and cyanotoxins removal by coagulation/flocculation: A review, Desalin. Water Treat. 20 (2010) 133–143. doi:10.5004/dwt.2010.1202.

[15] B. Naghavi, R.F. Malone, C. Station, B. Rouge, B. Rouge, Algae removal by fine sand/silt filtration, 20 (1986) 377–383.

[16] X. Zhao, Y. Zhang, Algae-removing and algicidal efficiencies of polydiallyldimethylammonium chloride composite coagulants in enhanced coagulation treatment of algae-containing raw water, Chem. Eng. J. 173 (2011) 164–170. doi:10.1016/j.cej.2011.07.058.

[17] S. Gao, M. Du, J. Tian, J. Yang, J. Yang, F. Ma, J. Nan, Effects of chloride ions on electro-coagulation-flotation process with aluminum electrodes for algae removal, J. Hazard. Mater. 182 (2010) 827–834. doi:10.1016/j.jhazmat.2010.06.114.

[18] S. Gao, J. Yang, J. Tian, F. Ma, G. Tu, M. Du, Electro-coagulation-

flotation process for algae removal, J. Hazard. Mater. 177 (2010) 336–343. doi:10.1016/j.jhazmat.2009.12.037.

[19] N. Uduman, V. Bourniquel, M.K. Danquah, A.F.A. Hoadley, A parametric study of electrocoagulation as a recovery process of marine microalgae for biodiesel production, Chem. Eng. J. 174 (2011) 249–257. doi:10.1016/j.cej.2011.09.012.

[20] G. Pérez, P. Gómez, R. Ibañez, I. Ortiz, A.M. Urtiaga, Electrochemical disinfection of secondary wastewater treatment plant (WWTP) effluent, Water Sci. Technol. 62 (2010) 892–897. doi:10.2166/wst.2010.328.

[21] D. Gášková, K. Sigler, B. Janderová, J. Plášek, Effect of high-voltage electric pulses on yeast cells: Factors influencing the killing efficiency, Bioelectrochemistry Bioenerg. 39 (1996) 195–202. doi:10.1016/0302-4598(95)01892-1.

[22] K.P. Drees, M. Abbaszadegan, R.M. Maier, Comparative electrochemical inactivation of bacteria and bacteriophage, Water Res. 37 (2003) 2291–2300. doi:10.1016/S0043-1354(03)00009-5.

[23] A.B. Boehm, Y. Cui, Conducting Nanosponge Electroporation for Affordable and High-Efficiency Disinfection of Bacteria and Viruses in Water, Nano Lett. (2013) 5–10.

[24] Y. Xu, J. Yang, M. Ou, Y. Wang, J. Jia, Study of *Microcystis aeruginosa* inhibition by electrochemical method, Biochem. Eng. J. 36 (2007) 215–220. doi:10.1016/j.bej.2007.02.022.

[25] W. Liang, J. Qu, L. Chen, H. Liu, P. Lei, Inactivation of *Microcystis aeruginosa* by Continuous Electrochemical Cycling Process in Tube Using Ti/RuO_2 Electrodes, 39 (2005) 4633–4639.

[26] M. Mascia, A. Vacca, S. Palmas, Electrochemical treatment as a pre-oxidative step for algae removal using *Chlorella vulgaris* as a model organism and BDD anodes, Chem. Eng. J. 219 (2013) 512–519. doi:10.1016/j.cej.2012.12.097.

[27] S. Ferro, A. De Battisti, I. Duo, C. Comninellis, W. Haenni, A. Perret, Chlorine evolution at highly boron-doped diamond electrodes, J. Electrochem. Soc. 147 (2000) 2614–2619. doi:10.1149/1.1393578.

[28] B. Marselli, J. Garcia-Gomez, P. -a. Michaud, M. a. Rodrigo, C. Comninellis, Electrogeneration of Hydroxyl Radicals on Boron-Doped Diamond Electrodes, J. Electrochem. Soc. 150 (2003) D79. doi:10.1149/1.1553790.

[29] A.M. Polcaro, A. Vacca, M. Mascia, F. Ferrara, Product and by-product formation in electrolysis of dilute chloride solutions, J. Appl. Electrochem. 38 (2008) 979–984. doi:10.1007/s10800-008-9509-3.

[30] M. Mascia, A. Vacca, S. Palmas, A.M. Polcaro, Kinetics of the electrochemical oxidation of organic compounds at BDD anodes: Modelling of surface reactions, J. Appl. Electrochem. 37 (2007) 71–76. doi:10.1007/s10800-006-9217-9.

[31] M.E.H. Bergmann, J. Rollin, Product and by-product formation in laboratory studies on disinfection electrolysis of water using boron-doped diamond anodes, Catal. Today. 124 (2007) 198–203. doi:10.1016/j.cattod.2007.03.038.

[32] I. Kolthoff, I. Miller, The chemistry of persulfate. I. The kinetics and mechanism of the decomposition of the persulfate ion in aqueous medium1, J. Am. Chem. Soc. 73 (1951) 3055–3059.

[33] P. Cañizares, C. Sáez, J. Lobato, M.A. Rodrigo, Electrochemical treatment of 2,4-dinitrophenol aqueous wastes using boron-doped diamond anodes, Electrochim. Acta. 49 (2004) 4641–4650. doi:10.1016/j.electacta.2004.05.019.

[34] K. Serrano, P.A. Michaud, C. Comninellis, A. Sa, Electrochemical preparation of peroxodisulfuric acid using boron doped diamond thin film electrodes, 48 (2002) 431–436.

[35] M.E.H. Bergmann, T. Iourtchouk, W. Schmidt, J. Hartmann, M.

Fischer, G. Nusske, D. Gerngrob, Laboratory- and technical-scale comparison of chlorate and perchlorate formation during drinking water electrolysis: a field study, J. Appl. Electrochem. 45 (2015) 765–778. doi:10.1007/s10800-015-0826-z.

[36] M.E.H. Bergmann, J. Rollin, T. Iourtchouk, The occurrence of perchlorate during drinking water electrolysis using BDD anodes, Electrochim. Acta. 54 (2009) 2102–2107. doi:10.1016/j.electacta.2008.09.040.

[37] D. Ghernaout, M.W. Naceur, A. Aouabed, On the dependence of chlorine by-products generated species formation of the electrode material and applied charge during electrochemical water treatment, Desalination. 270 (2011) 9–22. doi:10.1016/j.desal.2011.01.010.

[38] A.M. Polcaro, A. Vacca, M. Mascia, S. Palmas, J. Rodiguez Ruiz, Electrochemical treatment of waters with BDD anodes: Kinetics of the reactions involving chlorides, J. Appl. Electrochem. 39 (2009) 2083–2092. doi:10.1007/s10800-009-9870-x.

[39] A. Vacca, M. Mascia, S. Palmas, A. Da Pozzo, Electrochemical treatment of water containing chlorides under non-ideal flow conditions with BDD anodes, J. Appl. Electrochem. 41 (2011) 1087–1097. doi:10.1007/s10800-011-0274-3.

[40] L.R. Czarnetzki, L.J.J. Janssen, Formation of hypochlorite, chlorate and oxygen during NaCl electrolysis from alkaline solutions at an RuO_2/TiO_2 anode, J. Appl. Electrochem. 22 (1992) 315–324. doi:10.1007/BF01092683.

[41] S. Palmas, A.M. Polcaro, A. Vacca, M. Mascia, F. Ferrara, Influence of the operating conditions on the electrochemical disinfection process of natural waters at BDD electrodes, J. Appl. Electrochem. 37 (2007) 1357–1365. doi:10.1007/s10800-007-9368-3.

[42] M. Mascia, A. Vacca, A.M. Polcaro, S. Palmas, J.R. Ruiz, A. Da Pozzo, Electrochemical treatment of phenolic waters in presence of chloride with boron-doped diamond (BDD) anodes: Experimental

study and mathematical model, J. Hazard. Mater. 174 (2010) 314–322. doi:10.1016/j.jhazmat.2009.09.053.

[43] A.A. Mobarak, M.S.E. Abdo, M.S.M. Hassan, G.H. Sedahmed, Mass transfer behaviour of a flow-by fixed bed electrochemical reactor composed of a vertical stack of screens under single and upward two phase flow, J. Appl. Electrochem. 30 (2000) 1269–1276. doi:10.1023/A:1026537208886.

[44] M. Mascia, A. Vacca, S. Palmas, Fixed bed reactors with three dimensional electrodes for electrochemical treatment of waters for disinfection, Chem. Eng. J. 211–212 (2012) 479–487. doi:10.1016/j.cej.2012.09.091.

[45] I.R. Falconer, A.R. Humpage, Health risk assessment of cyanobacterial (blue-green algal) toxins in drinking water, Int. J. Environ. Res. Public Health. 2 (2005) 43–50. doi:10.3390/ijerph2005010043.

[46] W.M. Taama, R.E. Plimley, K. Scott, Mass transfer rates in a dem clectrochemical cell, Electrochim. Acta. 41 (1996) 543–548.

[47] T.R. Ralph, M.L. Hitchman, J.P. Millington, F.C. Walsh, Mass transport in an electrochemical laboratory filterpress reactor and its enhancement by turbulence promoters, Electrochim. Acta. 41 (1996) 591–603. doi:10.1016/0013-4686(95)00346-0.

[48] M. Griffiths, C.P. De León, F.C. Walsh, Mass transport in the rectangular channel of a filter-press electrolyzer (the FM01-LC reactor), AIChE J. 51 (2005) 682–687. doi:10.1002/aic.10311.

[49] M. Mascia, S. Monasterio, A. Vacca, S. Palmas, Electrochemical treatment of water containing *Microcystis aeruginosa* in a fixed bed reactor with three-dimensional conductive diamond anodes, J. Hazard. Mater. (2015). doi:10.1016/j.jhazmat.2016.03.004.

[50] S. Monasterio, F. Dessì, M. Mascia, A. Vacca, Electrochemical Removal of *Microcystis Aeruginosa* in a Fixed Bed Reactor, 41 (2014) 163–168. doi:10.3303/CET1441028.

[51] J.C. Weaver, Y.A. Chizmadzhev, Theory of electroporation : A review, 41 (1996) 135–160.

[52] H. Li, X. Zhu, J. Ni, Inactivation of *Escherichia coli* in Na_2SO_4 electrolyte using boron-doped diamond anode, Electrochim. Acta. 56 (2010) 448–453. doi:10.1016/j.electacta.2010.08.055.

[53] A.M. Polcaro, A. Vacca, M. Mascia, S. Palmas, R. Pompei, S. Laconi, Characterization of a stirred tank electrochemical cell for water disinfection processes, Electrochim. Acta. 52 (2007) 2595–2602. doi:10.1016/j.electacta.2006.09.015.

[54] Z. xing Wu, N. qin Gan, Q. Huang, L. rong Song, Response of *Microcystis* to copper stress - Do phenotypes of *Microcystis* make a difference in stress tolerance?, Environ. Pollut. 147 (2007) 324–330. doi:10.1016/j.envpol.2006.05.022.

[55] M.H. Park, I.M. Chung, A. Ahmad, B.H. Kim, S.J. Hwang, Growth inhibition of unicellular and colonial *Microcystis* strains (Cyanophyceae) by compounds isolated from rice (Oryza sativa) hulls, Aquat. Bot. 90 (2009) 309–314. doi:10.1016/j.aquabot.2008.11.007.

[56] M. Li, P.N. Nkrumah, Q. Peng, Different tolerances to chemical contaminants between unicellular and colonial morph of Microcystis aeruginosa: Excluding the differences among different strains, J. Hazard. Mater. 285 (2015) 245–249. doi:10.1016/j.jhazmat.2014.10.064.

[57] W. Dzwinel, K. Boryczko, D.A. Yuen, A discrete-particle model of blood dynamics in capillary vessels, J. Colloid Interface Sci. 258 (2003) 163–173. doi:10.1016/S0021-9797(02)00075-9.

[58] J. Sun, J. Wang, X. Pan, H. Yuan, A New Treatment Strategy for Inactivating Algae in Ballast Water Based on Multi-Trial Injections of Chlorine, (2015) 13158–13171. doi:10.3390/ijms160613158.

[59] C. Joannes, C.S. Sipaut, J. Dayou, S.M. Yasir, R.F. Mansa, Review Paper on Cell Membrane Electroporation of Microalgae using

Electric Field Treatment Method for Microalgae Lipid Extraction, IOP Conf. Ser. Mater. Sci. Eng. 78 (2015) 12034. doi:10.1088/1757-899X/78/1/012034.

[60] K.H.M. Cardozo, T. Guaratini, M.P. Barros, V.R. Falcão, A.P. Tonon, N.P. Lopes, S. Campos, M.A. Torres, A.O. Souza, P. Colepicolo, E. Pinto, Metabolites from algae with economical impact, Comp. Biochem. Physiol. - C Toxicol. Pharmacol. 146 (2007) 60–78. doi:10.1016/j.cbpc.2006.05.007.

[61] M. Di Lorenzo, K. Scott, T.P. Curtis, K.P. Katuri, I.M. Head, Continuous feed microbial fuel cell using an air cathode and a disc anode stack for wastewater treatment, Energy and Fuels. 23 (2009) 5707–5716. doi:10.1021/ef9005934.

[62] M. Di Lorenzo, A.R. Thomson, K. Schneider, P.J. Cameron, I. Ieropoulos, A small-scale air-cathode microbial fuel cell for on-line monitoring of water quality, Biosens. Bioelectron. 62 (2014) 182–188. doi:10.1016/j.bios.2014.06.050.

[63] M. Rahimnejad, A. Adhami, S. Darvari, A. Zirepour, S.-E. Oh, Microbial fuel cell as new technology for bioelectricity generation: A review, Alexandria Eng. J. 54 (2015) 745–756. doi:10.1016/j.aej.2015.03.031.

[64] T.H. Pham, K. Rabaey, P. Aelterman, P. Clauwaert, L. De Schamphelaire, N. Boon, W. Verstraete, Microbial fuel cells in relation to conventional anaerobic digestion technology, Eng. Life Sci. 6 (2006) 285–292. doi:10.1002/elsc.200620121.

[65] J. Chouler, G.A. Padgett, P.J. Cameron, K. Preuss, M.-M. Titirici, I. Ieropoulos, M. Di Lorenzo, Towards effective small scale microbial fuel cells for energy generation from urine, Electrochim. Acta. 192 (2016) 89–98. doi:10.1016/j.electacta.2016.01.112.

[66] D. Pant, G. Van Bogaert, L. Diels, K. Vanbroekhoven, A review of the substrates used in microbial fuel cells (MFCs) for sustainable energy production, Bioresour. Technol. 101 (2010) 1533–1543.

doi:10.1016/j.biortech.2009.10.017.

[67] N. Rashid, Y.F. Cui, S.U.R. Muhammad, J.I. Han, Enhanced electricity generation by using algae biomass and activated sludge in microbial fuel cell, Sci. Total Environ. 456–457 (2013) 91–94. doi:10.1016/j.scitotenv.2013.03.067.

[68] S.B. Velasquez-Orta, T.P. Curtis, B.E. Logan, Energy from algae using microbial fuel cells, Biotechnol. Bioeng. 103 (2009) 1068–1076. doi:10.1002/bit.22346.

[69] X.A. Walter, J. Greenman, B. Taylor, I.A. Ieropoulos, Microbial fuel cells continuously fuelled by untreated fresh algal biomass, Algal Res. 11 (2015) 103–107. doi:10.1016/j.algal.2015.06.003.

[70] H. Zheng, J. Yin, Z. Gao, H. Huang, X. Ji, C. Dou, Disruption of *Chlorella vulgaris* cells for the release of biodiesel-producing lipids: A comparison of grinding, ultrasonication, bead milling, enzymatic lysis, and microwaves, Appl. Biochem. Biotechnol. 164 (2011) 1215–1224. doi:10.1007/s12010-011-9207-1.

[71] E. Günerken, E. D'Hondt, M.H.M. Eppink, L. Garcia-Gonzalez, K. Elst, R.H. Wijffels, Cell disruption for microalgae biorefineries, Biotechnol. Adv. 33 (2015) 243–260. doi:10.1016/j.biotechadv.2015.01.008.

[72] E.M. Spiden, P.J. Scales, B.H.J. Yap, S.E. Kentish, D.R.A. Hill, G.J.O. Martin, The effects of acidic and thermal pretreatment on the mechanical rupture of two industrially relevant microalgae: Chlorella sp. and Navicula sp., Algal Res. 7 (2015) 5–10. doi:10.1016/j.algal.2014.11.006.

[73] J.J. Cole, Interactions Between Bacteria and Algae in Aquatic Ecosystems, Annu. Rev. Ecol. Evol. Syst., 13 (1982) 291-314. http://www.jstor.org/stable/209707.

[74] J. Winfield, I. Ieropoulos, J. Greenman, Bioresource Technology Investigating a cascade of seven hydraulically connected microbial fuel cells, Bioresour. Technol. 110 (2012) 245–250.

doi:10.1016/j.biortech.2012.01.095.

[75] L. Woodward, M. Perrier, B. Srinivasan, B. Tartakovsky, Maximizing Power Production in a Stack of Microbial Fuel Cells using Multiunit Optimization Method Maximizing Power Production in a Stack of Microbial Fuel Cells Using Multiunit Optimization Method, Biotechnol. Prog. (2009). doi:10.1021/bp.115.

[76] M.M. Ghangrekar, V.B. Shinde, Performance of membrane-less microbial fuel cell treating wastewater and effect of electrode distance and area on electricity production, Bioresour. Technol. 98 (2007) 2879–2885. doi:10.1016/j.biortech.2006.09.050.

[77] P. Ledezma, J. Greenman, I. Ieropoulos, MFC-cascade stacks maximise COD reduction and avoid voltage reversal under adverse conditions, Bioresour. Technol. 134 (2013) 158–165. doi:10.1016/j.biortech.2013.01.119.

Table of symbols

Roman symbols

A	Electrode area	(m^2)
a	Specific electrode area	(m^{-1})
	$a = {A}/{V_R}$	
A_{CELL}	Geometric area of the reactor	(m^2)
	$A_{CELL} = \pi \cdot ({d}/{2})^2$	
C_{AL}	Concentration of algae	(cells m^{-3})
C_i	Concentration of chemicals	(mol m^{-3})
D	Axial dispersion coefficient	(m^2 s^{-1})
d	Inner diameter of the reactor	(m)
d_p	Glass spheres dimension	(m)
E	Energy	(W h m^{-3})
$E(t)$	Exit age distribution	(s)
E_r	Energy requirement (batch system)	(kW h m^{-3})
E_{RW}	Energy requirement (continuous system)	(kW h kg^{-1})
F	Faraday number	96500 (A s mol^{-1})
i	Current density	(A m^{-2})
	$i = {I}/{A}$	

I	Current intensity	(A)
i_L	Limiting cahodic current density	(A m^{-2})
k_{app}	Apparent kinetic constant	(s^{-1})
k_i	Specific reaction rate	(s^{-1})
k_m^c	Cathodic mass transfer coefficient	(m s^{-1})
n_e	Number of electrons in an electrochemical reaction	
p	Parameter in equation (6)	
P	Volumetric power density	(W m^{-3})
q	Parameter in equation (6)	
Q	Electrolyte flow rate	(m^3 s^{-1})
R	Removal value between 0 and 1	
R_{ext}	Fixed external resistor	(Ω)
R_i	Kinetics equations	(mol m^{-3} s^{-1})
t_m	mean time	(s)
v	Electrolyte's velocity inside the reactor (no packing filling) $v = {Q}/{A_{CELL}}$	(m s^{-1})
V	System volume	(m^3)
V_R	Reactor volume	(m^3)
z	Axial coordinate (distance from the reactor inlet)	(m)

Greek symbols

ν	Kinematic viscosity of electrolyte	($m^2\ s^{-1}$)
ΔE_{CELL}	Cell potential	(V)
μ	Viscosity of electrolyte	($kg\ m^{-1}\ s^{-1}$)
ε	Bed void fraction	$\varepsilon = {V_R}/{V_{CELL}}$
ε_i	Fraction of current for the generation of the i^{th} compound	
λ	Chloprphyll-*a* pigment wavelength	(nm)
ρ	Density of electrolyte	($kg\ m^{-3}$)
σ^2	Variance of the peak	(s^2)
τ	Hydraulic residence time	(s)

Dimensionless numbers

Pe	Peclet number	$Pe = \frac{\nu \cdot d}{D}$
Re	Reynolds number	$Re = \frac{d \cdot \nu \cdot \rho}{\mu}$
Sc	Schmidt number	$Sc = \frac{\mu}{\rho \cdot D}$
Sh	Sherwood number	$Sh = \frac{k_m^c \cdot d}{D}$

Subscripts

A	Anode
C	Cathode
D	Decay
OX	Oxidant

Acronyms

$(NH_4)_6Mo_7O_{24}\cdot 4H_2O$	Ammonium molybdate tetrahydrate
AWW	Artificial wastewater
BDD	Boron Doped Diamond
$CaCl_2\cdot 2H_2O$	Calcium chloride dihydrate
Cl^-	Chloride ion
Cl_2	Chlorine gas
ClO^-	Hypochlorite ion
ClO_2	Chlorine dioxide
ClO_2^-	Chlorite ion
ClO_3^-	Chlorate ion
ClO_4^-	Perchlorate ion
COD	Chemical oxygen demand
$CuSO_4\cdot 5H_2O$	Copper (II) sulfate pentahydrate
CV	Cyclic Voltammetry
DE	Direct electrolysis
DPD	N,N-diethyl-p-phenylenediamine
DSA	Dimensionally Stable Anode
H^+	Hydron
H_2	Hydrogen
H_2O_2	Hydrogen peroxide
H_3BO_3	Boric acid

HCl	Hydrochloric acid
$HClO$	Hypochlorous acid
$HClO_2$	Chlorous acid
$HClO_3$	Chloric acid
$HClO_4$	Perchloric acid
$K_2HPO_4 \cdot 3H_2O$	Potassium hydrogen phosphate trihydrate
$K_3Fe(CN)_6$	Potassium ferricyanide
$K_4Fe(CN)_6$	Potassium ferrocyanide
KCl	Potassium chloride
LSW	Linear Sweep Voltammetry
MFC	Microbial Fuel Cell
$MgSO_4 \cdot 7H_2O$	Magnesium sulfate heptahydrate
$MnCl_2 \cdot 4H_2O$	Manganese (II) chloride tetrahydrate
Na_2CO_3	Sodium carbonate
$NaHCO_3$	Sodium bicarbonate
$NaNO_3$	Sodium nitrate
Nb	Niobium
$O^{\bullet}$	Oxygen radical
O_2	Oxygen
O_3	Ozone
OCV	Open circuit voltage
OH^-	Hydroxide

$OH^{\bullet}$	Hydroxyl radical
PDMS	Polydimethylsiloxane Silicon
RTD	Residence time distribution
$S_2O_8^{2-}$	Peroxydisulfate ion
SO_4^{2-}	Sulfate ion
UV	Ultraviolet
WW	Wastewater
$ZnSO_4 \cdot 7H_2O$	Zinc sulfate heptahydrate

List of figures[1]

Figures 1, 10, 11, 12, 16, 17, 18 and 19 from "Electrochemical treatment of water containing *Microcystis aeruginosa* in a fixed bed reactor with three-dimensional conductive diamond anodes", Journal of Hazardous Materials 319 (2016) 111-120, Permission requested.

Figures 13, 14, and 15 from "S. Monasterio, F. Dessì, M. Mascia, A. Vacca, S. Palmas, "Electrochemical removal of *Microcystis aeruginosa* in a fixed bed reactor", Chemical Engineering Transactions 41 (2014) 163–168.

List of tables[2]

Tables 5 and 6 from "Electrochemical treatment of water containing *Microcystis aeruginosa* in a fixed bed reactor with three-dimensional conductive diamond anodes", Journal of Hazardous Materials 319 (2016) 111-120, Permission requested.